

AD-A124 844

BODY FLAP HEAT TRANSFER DATA FROM SPACE SHUTTLE ORBITER 1/1

ENTRY FLIGHT TEST. (U) AIR FORCE INST OF TECH

WRIGHT-PATTERSON AFB OH SCHOOL OF ENGI.. J R WOOD

UNCLASSIFIED

DEC 82 AFIT/GA/AA/82D-12

F/G 22/2

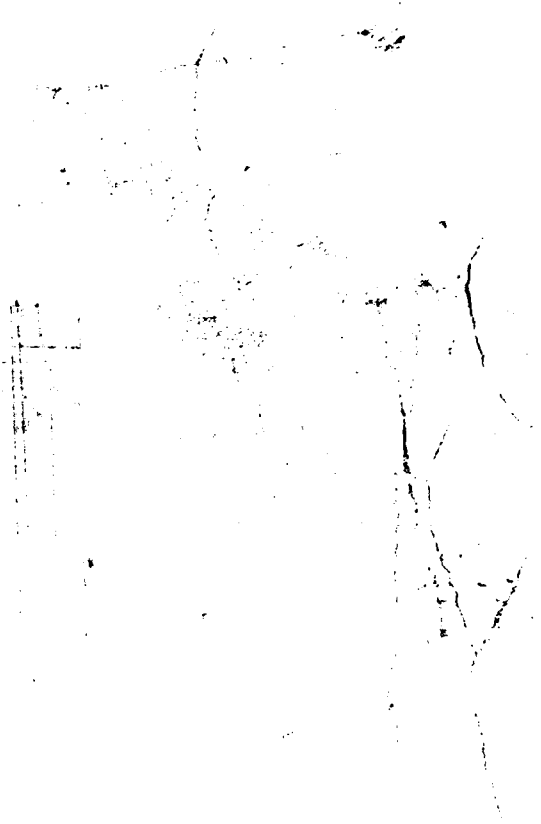
NL

END

FILMED

11

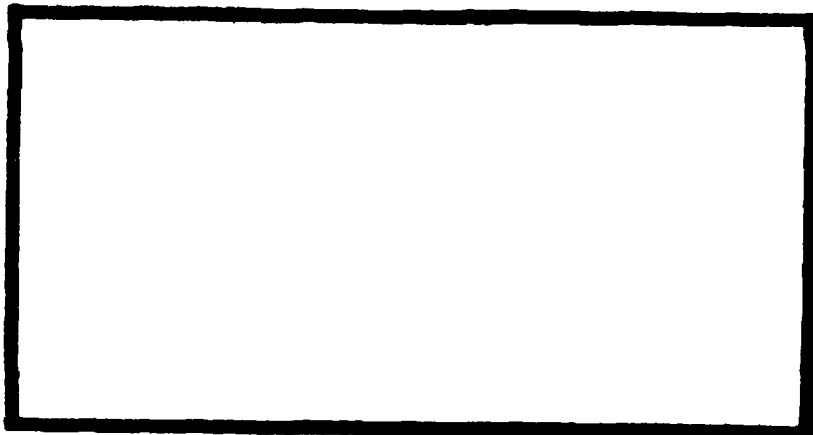
DTIC



1



AD A 124844



This document has been approved
for public release and sale; its
distribution is unlimited.

DTIC
SELECTED
FEB 23 1983
D

DEPARTMENT OF THE AIR FORCE
AIR UNIVERSITY (ATC)

AIR FORCE INSTITUTE OF TECHNOLOGY

Wright-Patterson Air Force Base, Ohio

DTIC FILE COPY

83 02 022 216

AFIT/GA/AA/82D-12

BODY FLAP HEAT TRANSFER DATA
FROM SPACE SHUTTLE ORBITER
ENTRY FLIGHT TEST MANEUVERS

THESIS

AFIT/GA/AA/82D-12

John R. Wood
Capt USAF

DTIC
FEB 23 1983

A

Approved for public release; distribution unlimited

AFIT/GA/AA/82-12

BODY FLAP HEAT TRANSFER DATA
FROM SPACE SHUTTLE ORBITER
ENTRY FLIGHT TEST MANEUVERS

THESIS

Presented to the Faculty of the School of Engineering
of the Air Force Institute of Technology
Air University
in Partial Fulfillment of the
Requirements for the Degree of
Masters of Science

by

John R. Wood, B.S.

Capt. USAF

Graduate Astronautical Engineering

December 1982

Accession For	
NTIS GRA&I	<input checked="" type="checkbox"/>
DTIC TAB	<input type="checkbox"/>
Unannounced	<input type="checkbox"/>
Justification	
By	
Distribution/	
Availability Codes	
Dist	Avail and/or Special

Approved for public release; distribution unlimited

Acknowledgements

When it came to selecting a thesis topic, my hope was to do something related to or about the Space Shuttle. I was fortunate that in January 1982, Capt Jim Hodge came to teach at AFIT from the Air Force Flight Test Center with many unanswered questions about the Space Shuttle Orbiter reentry heating affects which may be of great concern to future Air Force and NASA mission planning. Despite my lack of knowledge in several areas concerning this project, instruction and assistance from Capt Hodge on the use of the AFFTC HEATEST program, from Dr. Will Hankey in the fundamentals of high speed aerodynamics, and from Capt David Audley in the fundamentals of Systems Identification theory made completion of this thesis possible. My special thanks to them, to the rest of the Engineering and Math department faculty at AFIT, to my classmates, to my friends and family for their spiritual support, to the Air Force for permitting me to be here, and to God who receives all the glory for the things He has done for me.

I sincerely hope this will be of benefit to future investigators of the Orbiter reentry aerodynamics.

John R. Wood

List of Figures

Figure		Page
1	Space Shuttle Orbiter	2
2	Systems Approach to Envelope Expansion	5
3	Body Flap	10
4	Simplified HEATEST Flow Diagram	14
5	TPS Model Cross Section	17
6	Body Flap Thermocouple Temperature History During STS-2, 3, and 4 Reentries	23
7	Body Flap, Elevon, and Angle of Attack Variation During STS-2 Flight Test Maneuvers	25
8	Body Flap and Elevon Deflections for Att Orbiter CG at Mach 18	27
9	Body Flap and Elevon Deflections for Nominal Orbiter CG at Mach 18	28
10	Derivatives and Error Bounds From HEATEST	33
11	Q Verses $\log Re$ $\log Re$	35
12	Q/Q_{ref} Verses $\log Re$ For Flight Data and Reynold's Analogy	37
13	Q/Q_{ref} Versus $Re^{1/2}$ For Flight Data and Calculated Heating Models	41
14	Reynold's Analogy, Eckert, Stanton Number Enthalpy, and Flight Data Q/Q_{ref} Verse Re	42
15	Wind Tunnel, NASA and Weak Shock Models and Flight Data Q/Q_{ref} Verses Body Flap Deflection	43
16	ΔQ Stagnation Verses $Re^{1/2}$ Using RC Approximation	49
17	ΔQ Eckert Verses $Re^{1/2}$ Using RC Approximation	51
18	Q/Q_{ref} Stagnation and Eckert in HEATEST	55

List of Tables

Table		Page
1	STS-2 Flight Test Maneuver Key Events	26
2	Entry Reference Conditions For Heating Method Calculations	61
3	Method 1. Calculations Using Reynold's Analogy and Sutherland's Law	63
4	Method 2. Calculations Using Normal Shock Tables Rockwell Normal Shock Approach	65
5	Method 3. Weak Shock Approximation Using $M_2=3$. .	67
6	Method 4. Newtonian Flow Analysis	69
7	Method 5. Eckert Flat Plate Analysis	70
8	Method 6. Calculations For Stanton Number-Enthalpy Analysis	71
9	Method 7. Spalding and Chi Cf Analysis and its Effect On Stanton Number-Enthalpy Values	73

List of Symbols

A	area
C,Cp	specific heat
C	skin friction coefficient
C	pitching moment coefficient
G	kalman gain
h	enthalpy
J	approximation of Jacobian
K_A, \dots, K_D	thermal conductivity in block A, ..., D
L	total number of spatial node points
M	Mach number
N	total number of thermocouple time samples
Nu	Nusselt number
P	pressure
Q	heating rate
Qref	reference heating rate
R	recovery factor
Re	Reynold's number
S	"score" in HEATEST model
t	entry time, measured from 122 km (400,000 ft)
T	temperature
V	relative velocity
x	axial distance from nose of Orbiter (for the location studied in this report, =107.5 ft)
α	angle of attack, degrees
ϕ	angle of sideslip, degrees
δ	deflection angle, degrees

List of Symbols

ϵ	emissivity
Θ	model parameters (vector of length K)
ρ	density
μ	viscosity
σ	Stefan-Boltzmann constant

Superscripts

+	a posteriori update
-	a priori propagation
*	best estimate

Subscripts

aw	adiabatic wall
i,j	number of spatial node points
k	number of model parameters
m	number of thermocouples
n	number of time steps
o	initial conditions
t	total
w	wall
∞	freestream conditions
1	conditions upstream of a shockwave
2	conditions downstream of a shockwave
A,...,D	in block A,...,D
FACE	body flap face sheet
HC	body flap honeycomb material
SIP,RTV	TPS Strain Isolation Pad and Room Temperature Vulcanizing adhesive material

Contents

	Page
Acknowledgements	ii
List of Figures	iii
List of Tables	iv
List of Symbols	v
Abstract	ix
I. Introduction	1
Background	1
The AFFTC Role	1
AFFTC Models	1
The Flight Test Maneuvers	4
Problem and Scope	7
II. The Space Shuttle Body Flap and TPS Operation	9
General Description	9
Body Flap Operation	9
TPS on the Body Flap	12
III. The HEATEST Program	13
Heating Model	13
Thermal Model	16
Use of the RC Circuit Analogy and Time Constant in HEATEST	20
IV. Flight Test Maneuvers	22
Objectives	22
Performance of Maneuvers on STS-2 and 4	27
V. Results	30
Initial Computer Runs and Analysis	30

Contents(cont.)

	Page
Comparison of Heating Models	36
Input of Models into HEATEST	46
VI. Conclusions	55
VII. Recommendations	56
Bibliography	58
Appendix A: Derivation of Heating Model Solutions . .	60
Appendix B: RC Circuit Analogy	74
Vita	76

Abstract

The Space Shuttle Orbiter has conducted various flight test maneuvers during the Orbital Flight Test Program and beyond in order to establish heating rates at various angles of attack and center of gravity positions. The objective of this project was to investigate the heating effects on the body flap during the entry flight test maneuvers and determine the limits on the flap deflections for an aft center of gravity envelope on the Orbiter.

An analysis program available from the Air Force Flight Test Center (AFFTC) uses applicable simulation equations for the aerodynamic performance of the TPS in their flight simulator and data reduction program (HEATEST). The approach was to use the HEATEST program to determine the heating on one critical point on the body flap during the STS-2 entry flight test inputs (Flap Thermocouple #V07T9508). From these results and other results on the outboard elevons, the maximum flap deflection angle and Orbiter aft center of gravity could be established.

Using the HEATEST program, results were obtained for angle of attack and body flap deflection effects but difficulty was encountered with Reynold's number effect. Several theoretical approaches were investigated resulting in at least one technique that could be applied to HEATEST to linearize or eliminate the Reynold's number effect.

BODY FLAP HEAT TRANSFER DATA
FROM SPACE SHUTTLE ORBITER
ENTRY FLIGHT TEST MANEUVERS

I. Introduction

Background

The United States Space Transportation System, the Space Shuttle, has presented aerodynamicists with a unique new challenge. Development of the entry flight characteristics and range of operations of its primary component, the Orbiter, seen returning in Fig. 1, is vital to the overall success of its mission. A systematic approach of integrating the best of ground tests, flight simulations, and flight tests needed to be developed.

The AFFTC Role

The Air Force Flight Test Center (AFFTC) has been and is continuing to conduct an evaluation of the Orbiter to assess its capability to meet Department of Defense requirements. The goal of the evaluation is to identify and remove placards in the Orbiter's operational envelope that could affect nominal and contingency landing operations from Vandenberg Air Force Base, California, which are more severe than the present launch and landing mode.

AFFTC Models

Equations and parameters were chosen to create aerodynamic heating and one-dimensional thermal models for the

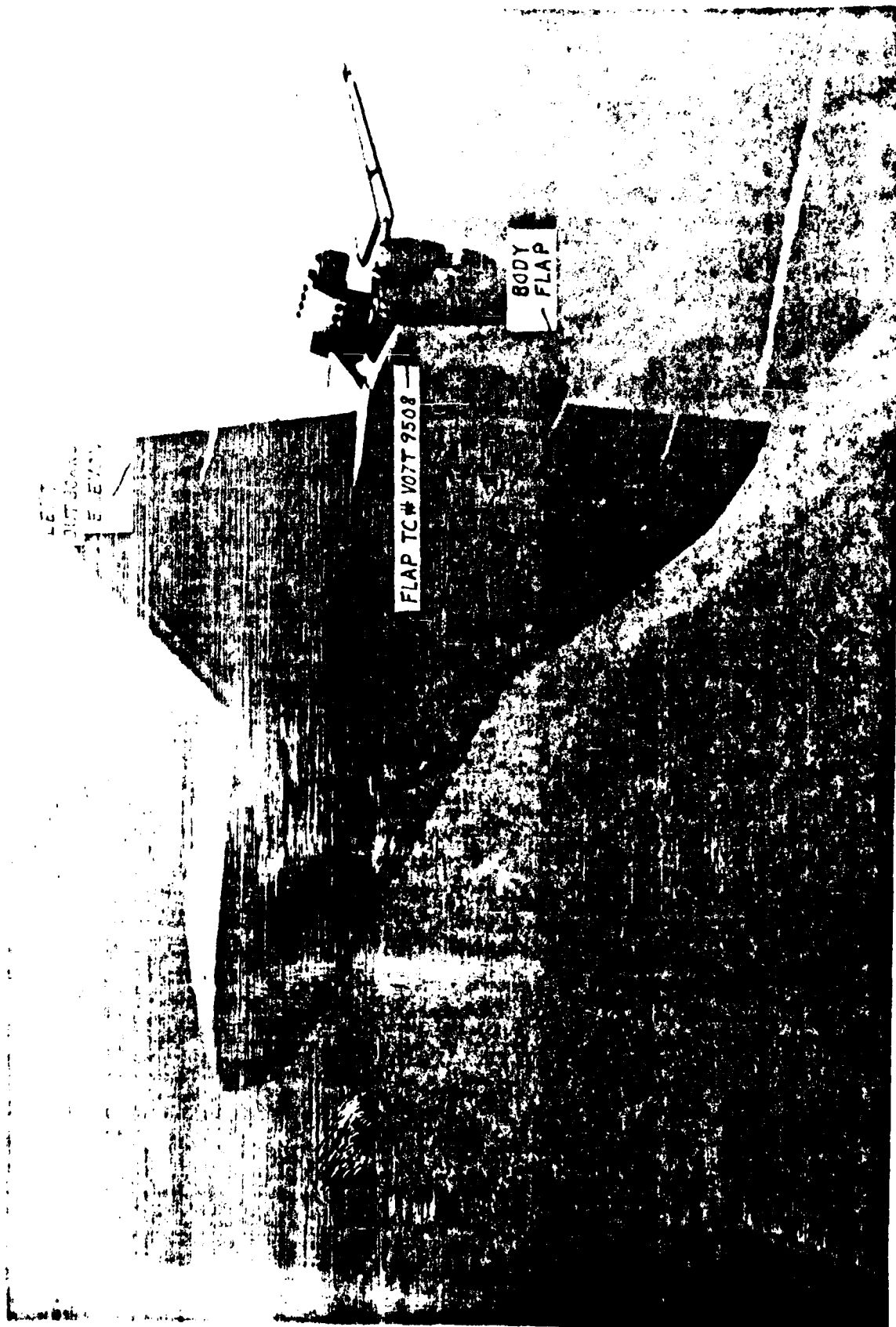


Figure 1. Body and flap of the

AFFTC flight simulator (Ref 1). The simulator was also used for flight planning and the design of flight test maneuvers to enhance flight test data reduction for angle of attack and center of gravity envelope expansion. Rapid expansion of the flight envelope is required prior to more severe entry conditions and prior to removal of the flight test data instrumentation from the operational vehicles. Upon obtaining embedded thermocouple data, a reduction technique based on systems identification theory was employed (Ref 2).

In systems identification theory, models are simulation equations and parameters required for aerothermodynamic performance of the Orbiter's Thermal Protection System (TPS). The AFFTC simulator data base goes beyond the simple use of a sphere (Ref 3) to determine reference heating conditions and employs models to determine the variations associated with angle of attack (α), elevon and body flap deflections (δ_e and δ_{bf}), Reynold's and Mach number (Re), and sideslip (ϕ).

A program called HEATEST (for HEAT ESTimation) was used to reduce the flight data. The variations above were assumed to be linear derivatives of the heat rate. Using a heating model the simulator was used to calculate a nondimensional heating ratio. A thermal model was also used within the program to calculate the temperature through the TPS. The one-dimensional differential equations in this thermal model are solved numerically to propagate the temperature, sensitivity of the temperature to each parameter, and the covariance of the temperature to the next discrete time at discrete node points through the TPS (Ref 1).

The Flight Test Maneuvers

The flight test maneuvers employ two techniques to obtain the envelope expansion data. A block diagram of this approach is shown in Fig. 2 (Ref 1). The first, called a Push-Over, Pull-Up (POPU), is employed at a prescribed velocity during the Orbiter entry when, from a given angle of attack, it is pitched downward manually by the crew at a preplanned rate, held at the minimum angle of attack for five seconds, then pitched upward to a maximum angle of attack and again held for the same duration before being brought back to its original position. This maneuver is employed to obtain aerodynamic lift to drag ratio and vehicle trim information as a function of the angle of attack. With deviations in the flight path of opposite signs and by holding the maneuver to only a few seconds the original trajectory is not significantly affected while at the same time AFETC simulator studies have indicated that most thermocouple locations would be affected. With other variables constant, the heating rate versus angle of attack derivative (Q_α) could be estimated by thermocouple measurements.

A second type of maneuver called a body flap sweep consists of cycling the body flap up and down while other variables are constant. A roll doublet can also be performed while the flap is down and the elevon is up to estimate aileron control derivatives.

Several considerations must be made in determining the mission entry profile. A steeper entry could be performed causing higher reference heating but over a shorter period of

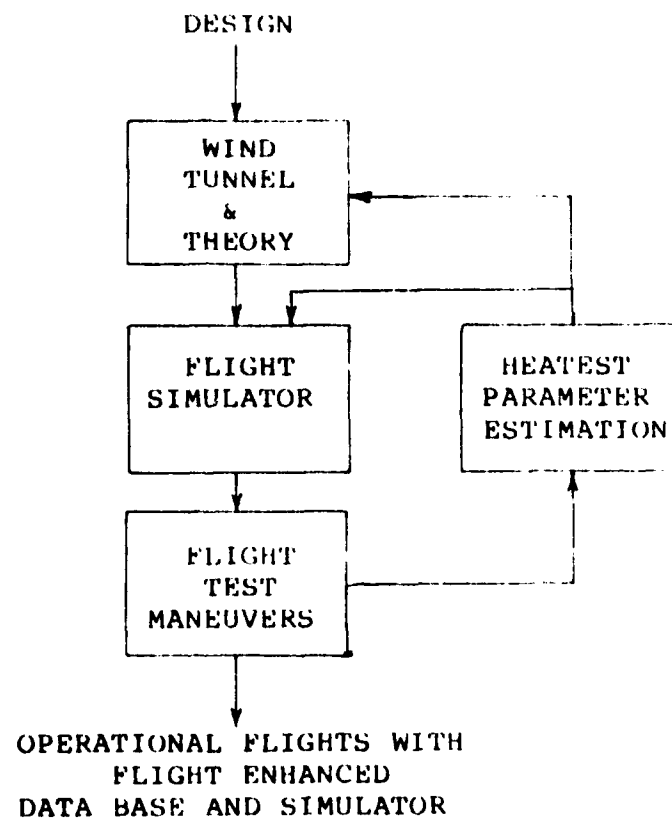


Figure 2. Systems Approach To Envelope Expansion

time than the shallow entry that produces lower peak heating, but higher total heating. Another consideration is the flap and elevon schedule. If the flap starts at a low (near zero) deflection angle it should increase in positive deflection (downward) to maintain trim. At the hinge line, the previously heated section of the flap now begins to become part of the hinge area and radiates heat to the aluminium chain seal, rib plate, and other internal areas in the aft fuselage possibly creating a heating problem. So the preferred deflection schedule for the body flap is to have a high positive deflection and decrease during entry. However, a trade off must be made here with the elevons which deflect to balance the trim. They also heat at higher deflections and must be used for banking and angle of attack control.

Execution of the flight test maneuvers was successfully carried out on the second, third, and fourth shuttle missions; STS-2, 3, and 4. STS-2 performed a series of maneuvers; a POPU at Mach 20 and three flap maneuvers at Mach 21, 17, and 14 as well as other aerodynamic maneuvers. The HEATEST program was used to determine the heating derivatives at most key locations on the Orbiter. No problems were encountered in estimating derivatives during the POPU at points on the lower surface from the nose to X/L of .7. The upper surface derivatives also were determined for the Orbital Maneuvering System (OMS) pods. Problems at a point on the elevons and of higher than anticipated heating at one point on the OMS pods were encountered but were resolved by HEATEST after some manipulation.

Problem and Scope

The body flap data, the heating effects on it, and its affect on the limits of the aft Center of Gravity (CG) of the Orbiter had not been fully reduced until this report. The approach in reducing this data was to use HEATEST as previously accomplished for other Orbiter locations. This was done by estimation of the heating and thermal parameters for various Mach number conditions during the timeframe when the maneuvers were taking place. The program was run in segments to identify heat estimates and determine their trends throughout the entry. After these estimates and their error bounds were determined, a similar procedure was to be used on another body flap thermocouple to determine its effects. Then, by combining these results with results obtained on the elevon heating at the same time, an estimate of the heating limits of the elevon and body flap deflections could be obtained. From these estimates a nominal and maximum aft CG limit for various angle of attack conditions during entry could be produced. This could establish a baseline for limits (as now perceived) to the maximum crossrange of the Orbiter based on heating and thermal parameters.

This report describes the Space Shuttle Orbiter body flap and its TPS operations during entry. It also explains the theory relevant to the body flap calculations in the HEATEST program. A detailed analysis of the performance of the flight test maneuvers conducted thus far and the resultant heating on the body flap thermocouple under study is included. Results obtained from these maneuvers in relation to

deviation of the basic pitching moment from pre-flight STS-1 estimates is also shown.

Finally, the results of the analysis of the heating and thermal parameters is discussed as well as the problems encountered at this point in the analysis. Alternative approaches and final results, conclusions, and recommendations complete this report.

II. The Space Shuttle Body Flap and TPS Operation

General Description

The body flap is an integral part of the Orbiter as seen on Fig. 3. It consists of an aluminum structure, ribs, spars, honeycomb, skin panels, and a trailing edge assembly. The main upper and lower forward honeycomb skin panels are joined to the ribs, spars, and honeycomb trailing edge with structural fasteners. The removable upper forward honeycomb skin panels complete the body flap structure. The body flap is covered with High Temperature Reuseable Surface Insulation (HRSI) and an articulating pressure and thermal seal to its forward cover area on the lower surface of the body flap to block heat and air from penetrating to the structure. The body flap deflects from the hinge line. Physically, the body flap can deflect +22.5 degrees (downward) and -11.7 degrees (upward) from the hinge line. However, the base of the aft fuselage angles upward approximately 5.5 degrees in relation to the rest of the base so the angle the flap deflects is not the same as its deflection angle in relation to the flow passing under the rest of the Orbiter's base.

Body Flap Operation

The two primary functions of the body flap are to protect the Space Shuttle Main Engine's (SSME's) from entry heating and to act in conjunction with the elevons as a center of gravity trim device. The Orbiter is a unique vehicle in that it is the first manned vehicle to reenter the atmosphere.

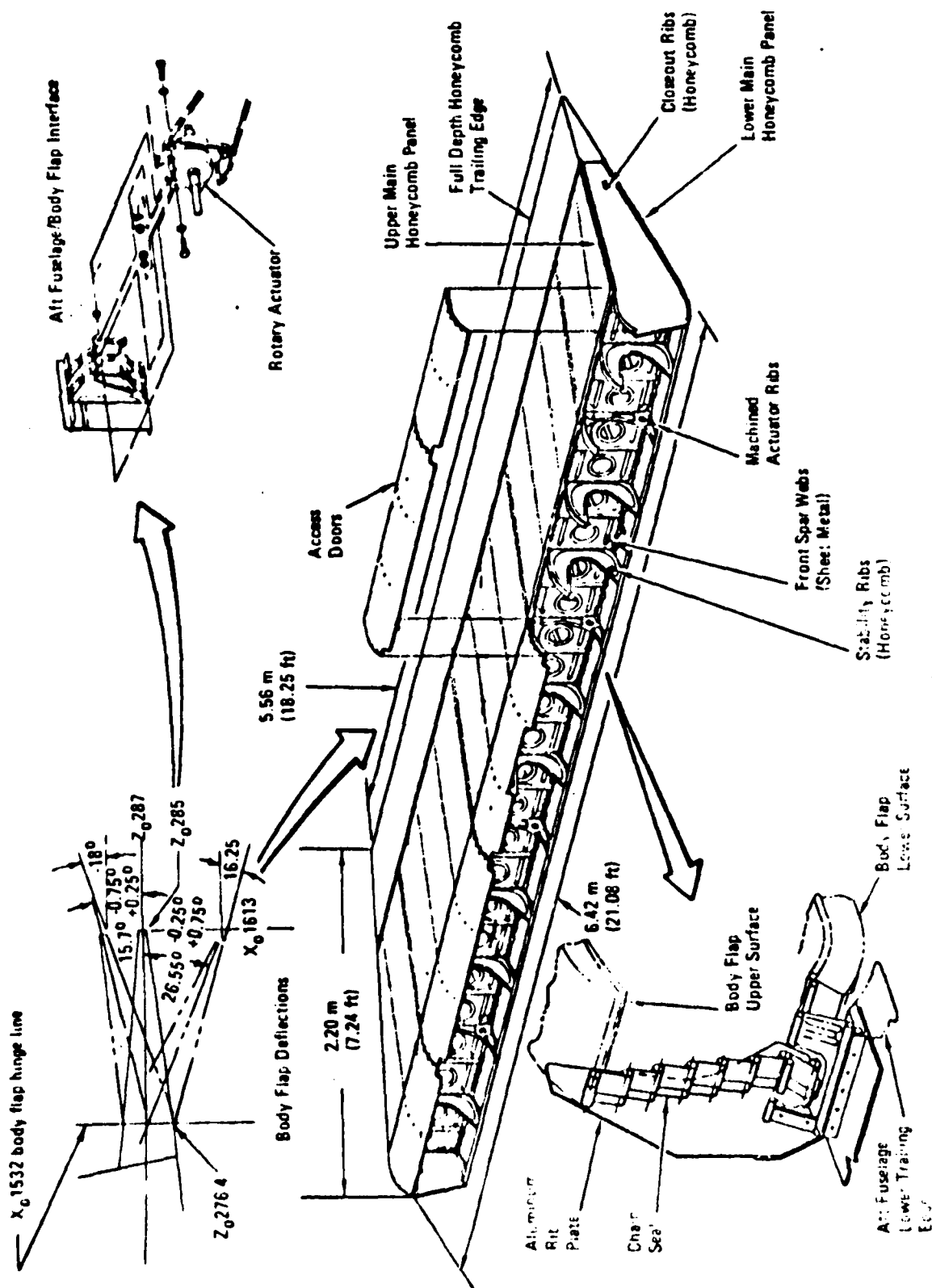


Figure. 3 Body Flap

like a glider. The angle of attack during entry is dictated by the mission requirements. The Orbiter was designed to have a 980 nautical mile cross-range maneuvering capability. Since DOD planned launches from the Western Test Range at Vandenberg AFB presently need this capability to fulfill their nominal and Abort Once Around requirements, the Orbiter must enter at an angle of attack of 36 to 38 degrees and roll angle of 60 degrees. Later in the entry, to obtain more cross-range by increasing the lift to drag ratio, the angle of attack is reduced to as low as 26 degrees. Unfortunately, this also severely increases the heating at many locations including the flap. This is due to higher Reynold's number and body flap deflection at lower angle of attack. The flap deflects more to maintain trim at lower angles of attack. The Reynold's number increase is due to a higher velocity and density with the lift coefficient rising faster than the drag coefficient at a lower altitude in the flight corridor. Later in the entry a gradual pitch down is initiated starting below Mach 8.

The elevons and body flap also must be used together to control the trim of the Orbiter during the entry period. The nominal CG position is .667 from the nose tip while the most aft CG position is .675. The aft CG increases body flap deflection (δ_{ff}) and elevon deflection (δ_e) for trim. It is therefore important to know the heating rates on the body flap and elevons at various deflections to determine if the reuseable surface insulation on both can protect them and be reused.

The TPS on the Body Flap

The Thermal Protection System (TPS) on the Orbiter was designed to protect the Orbiter and still be reusable for at least one hundred missions. The TPS on the Orbiter consists primarily of four types of materials, each designed to insulate the Orbiter's aluminum skin. The High Temperature Reusable Surface Insulation (HRSI) is able to withstand temperatures as high as 2600 F for one mission and be reusable when not exposed to temperatures higher than 2270 F. The tile consists of amorphous borosilicate glass. To prevent damage to the fragile tile, strips of felt padding are used between the tiles and the Orbiter's skin. This Strain Isolation Pad (SIP) is bonded to both the tile and the orbiter with a red, room-temperature vulcanizing (RTV) cement with an iron oxide base. Other strips of padding called filler bars are placed between each tile.

III. The HEATEST Program

Heating Model

A program named HEATEST (for HEAT ESTimating) was used to reduce flight test data. A flow chart of HEATEST is depicted in Fig. 4. HEATEST incorporates systems theory of theoretical models in order to compute parameters that effect the heating. The theory from scientific method has established a linearly independent set of parameters. Due to the number of these parameters, the systems theory in HEATEST combines some of these variations in order to compute them quickly. The variations are assumed to be linear derivatives of the heat rate. The heating ratio Q/Q_{ref} was assumed to be

$$Q/Q_{ref} = f(\alpha, \beta, \delta, Re) \quad (1)$$

where Q_{ref} is the dimensionless reference heat rate on a one foot diameter sphere given by

$$Q_{ref} = 17700 \sqrt{\rho_{\infty}} (V_{\infty}/10^4)^{3.67} (1-Hw/Ho) \quad (2)$$

$$hw = .24 [Q_{ref}/(\sigma \epsilon)]^{.25} \quad (3)$$

$$ho = .24 T_{\infty} + V_{\infty}^2/50063 \quad (4)$$

where the heating rate is in British Thermal Units (BTU's) per foot squared per second, σ is the Stefan-Boltsman constant (4.761×10^{-12}), ϵ is the emissivity, ρ_{∞} is the atmospheric density in slugs per cubic foot, V_{∞} is the relative velocity in feet per second, and T_{∞} is the atmospheric temperature in degrees Rankine.

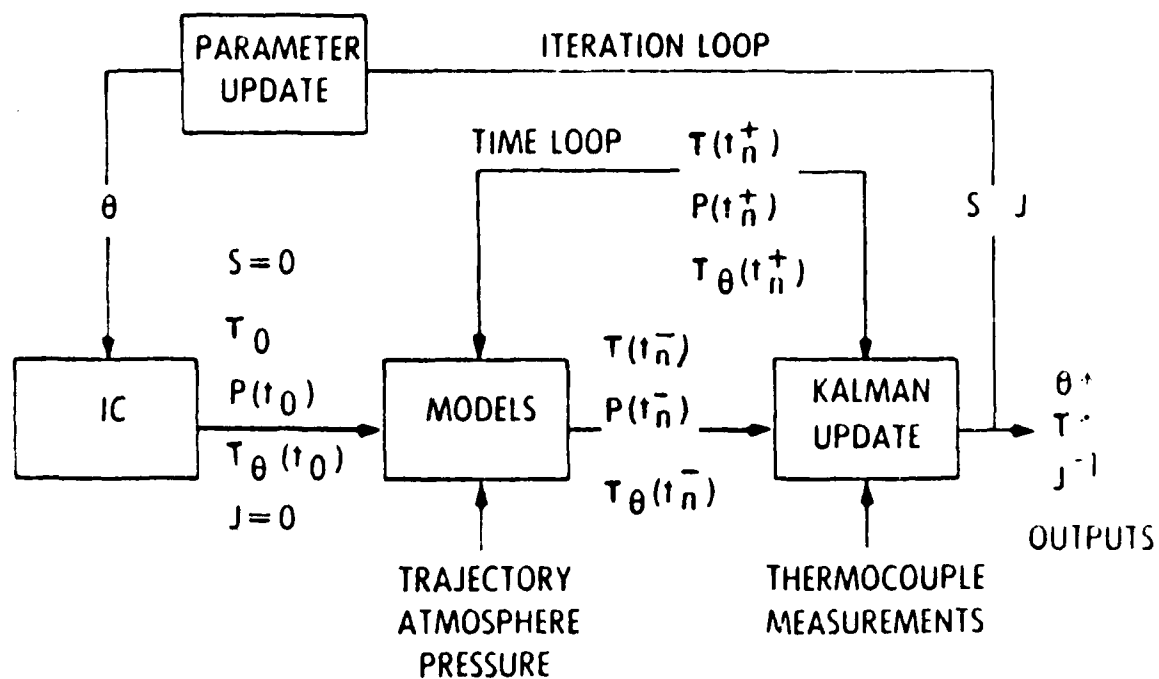


Figure 4. Simplified HEATEST Flow Diagram

This heating model and wind tunnel data at specific Orbiter TPS points were used to calculate the simulator heating rate ratio using linear interpolation routines for real-time processing of aerodynamic data. For the HEATEST data reduction program the heating ratio took the form

$$\begin{aligned} Q = Q/Q_{ref} = & Q_0 + Q_{\alpha}(\alpha - \alpha_0) + Q_{\beta}(\beta - \beta_0) \\ & + Q_{\delta_{ef}}(\delta_{ef} - \delta_{ef_0}) + Q_{\delta_e}(\delta_e - \delta_{e_0}) \\ & + Q_{\log Re} [\log(Re) - \log(Re_0)] \\ & + Q_M(M_{\infty} - M_{\infty_0}) \end{aligned} \quad (5)$$

where Q_0 is the magnitude at the reference conditions specified by the variables with the zero subscripts. In the body flap calculations the β terms and M terms were neglected. The subscripts on the heating ratio (Q) represent partial derivatives with respect to the variables of angle of attack (α), sideslip (β), the logarithm to the base ten of the Reynold's number (Re) based on its characteristic length, elevon deflection angle (δ_e), body flap deflection angle (δ_{ef}), and Mach number (M_{∞}).

These heating derivatives are essential in the evaluation of determining what factors influence the entry heating at the flap. Another value of Q_{ref} could be

$$Q_{ref} = .332(T_o - T_w)Re^{-.5} \rho_{\infty} V_{\infty} C_p / (778.3 Pr^{.2/3}) \quad (6)$$

which is based on Eckert theory for laminar flow with no deflection. Laminar flow is appropriate for most areas on the Orbiter. However, as will be later demonstrated, it is not correct for the flap and other regions where the turbulent

equation for the deflection

$$Q_{ref} = .0296(T_o - T_w) Re^{-.5} V_{\infty} C_p (T^*/T_o)^{.6} / (778.3 Pr^{.2/3}) (P/P_{\infty}) \quad (7)$$

and the T^* value is

$$T^* = T_2 + .5(T_w - T_2) + .22(TR - T_2) \quad (8)$$

is more representative of the heating. TR is assumed as $.9T_o$.

The change in the heat rate (ΔQ) from the reference conditions is given by

$$\Delta Q = Q - Q_o \quad (9)$$

where the magnitude of the reference condition is subtracted. The assumption is made that for short time segments these derivatives are constant and the lateral conduction in each tile is small.

Thermal Model

The AFPTC simulator also employs a thermal model of the TPS tile to calculate the temperature at various locations within the tile and its surroundings. A description of this model is shown in Fig. 5. The interior of the tile is divided into equal thickness and the entire structure of different materials is designated by blocks. Numerical solution of the resulting equations resulted in an accurate simulation of surface and bondline temperatures at specific locations. The honeycomb also is included in this analysis. There are two face sheets on the honeycomb with very little aluminum in between so that there is radiative heat transfer caused by the

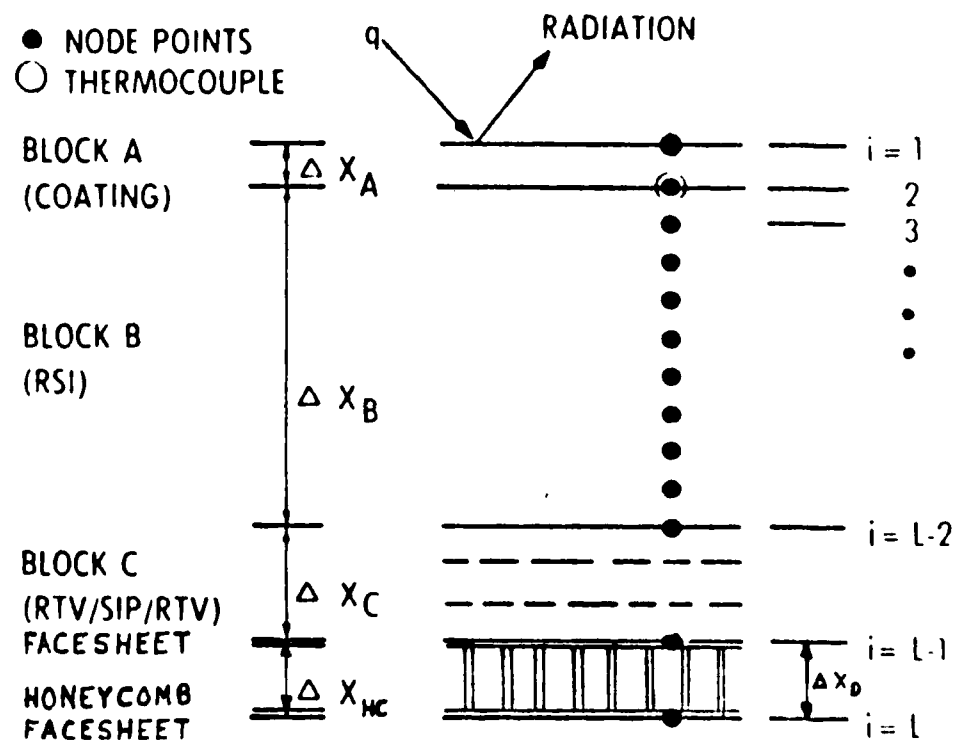


Figure 5. TPS Model Cross Section

different temperatures between the two sheets. If it is assumed that there is no material present, then in it is only the radiation between the two node points or

$$(1-A)\epsilon\sigma(T_i^4 - T_\infty^4) \quad (10)$$

where A is area per unit area aluminum between the facesheets.

In the tile, node points are spaced equally into small elements of length ΔX for a total of L node points. Each block has four equally spaced nodes. Each block represents a different material with different properties. Although thermocouples can be placed at various node points in each block, for our purposes the only thermocouple is located at the second node ($i=2$) which is ΔX_a from the surface. The convective heat rate (Q) input at node 1 has most of the heat radiated away and conducts a small amount to node 2 and the rest of the tile. Block C is bonded to the tile by RTV adhesive to the SIP which is also attached to the honeycomb face sheet by RTV.

An ordinary differential equation for the temperature (T_i) at the i th node point was obtained from an energy balance for each element. A system of L nonlinear differential equations results (Ref 1).

The energy balances for each element are summed together to form the heat transfer equations (Ref 4)

$$i=1 \quad (C_A \rho_A \Delta X_A / 2) T = -K_A / \Delta X_A T_1 + K_A / \Delta X_A T_2 \quad (11) \\ -\sigma\epsilon(T_i^4 - T_\infty^4) + f(\alpha, \beta, \delta, Re) Q_{ret}$$

$$i=2 \quad (C_A f_A \Delta X_A / 2 + C_g f_g \Delta X_2 / 2) \dot{T}_2 = K_A / \Delta X_A T_2 - (K_A / \Delta X_A + K_A / \Delta X_A) T_2 + K_g / \Delta X_2 T_3 \quad (12)$$

$$i \quad C_g f_g (\Delta X_{i-1} + \Delta X_i) / 2 \dot{T}_i = K_g / \Delta X_{i-1} T_{i-1} - (K_g / \Delta X_{i-1} + K_g / \Delta X_i) T_i + K_g / \Delta X_i T_{i+1} \quad (13)$$

$$i=L-2 \quad (C_g f_g \Delta X_{L-3} / 2 + C_c f_c \Delta X_c / 2) \dot{T}_{L-2} = K_c / \Delta X_c T_{L-3} - (K_g / \Delta X_{L-3} + K_c / \Delta X_c) T_{L-2} + K_c / \Delta X_c T_{L-1} \quad (14)$$

$$i=L-1 \quad (C_{SIP} f_{SIP} \Delta X_{SIP} / 2 + C_{RTV} f_{RTV} \Delta X_{RTV} + C_{HC} f_{HC} \Delta X_{HC} A / 2) \dot{T}_{L-1} = K_D / (\Delta X_c) T_{L-2} - (K_D^+ + K_D^-) T_{L-1} + K T_L + \epsilon_{HC} \sigma ([T_L + 460]^4 - [T_{L-1} + 460]^4) (1-A) \quad (15)$$

$$i=L \quad (C_{HC} f_{HC} \Delta X_{FACE} + C_{HC} f_{HC} A X_{HC} / 2 + C_D f_D (\Delta X_D / 2 + \Delta X_{SINK}) \dot{T}_L = \epsilon_{RAD} \sigma ((T_L + 460)^4 - (T_\infty + 460)^4) - HF (T_L + 460 - T_\infty) + K_D^- T_{L-1} - K_D T_L + \epsilon_{HC} \sigma ([T_L + 460]^4 - [T_{L-1} + 460]^4) (1-A) \quad (16)$$

The thermal conductivity (K) is a function of temperature and local pressure. The conductivity is evaluated at an average temperature between the nodes. The specific heat (C) is also dependent on the temperature at the node point. The dot represents the time rate of change of the temperature (Ti) at each node with a distance (ΔX_i) between each node and is approximated by a first order backward difference.

If the surface conditions can be specified, i.e. the thermal emissivity (ϵ), the coating thickness (ΔX_a), and the aerodynamic heating rate $t(\alpha, \beta, \delta, Re)$, the temperature through the tile can be calculated by solving the system of ordinary

differential equations. The specific heat and density (ρ) are assumed to be known from the design but emissivity can vary from .75 to .92 and the thermal conductivity (a function of tile pressure) is variable with flight pressures inside the tile in doubt (Ref 1 and 4). Using a stochastic estimation process the unknown parameters are found from systems identification theory.

All temperatures at each node through the TPS are not measured in the previous described model because thermocouples are not located at each node point. Thus an intermediate step uses an extended Kalman filter to estimate all node temperatures whenever a thermocouple sample was available. This was based on the thermocouple measurement and heating, thermal, and error models. This filter also filtered out noise. The parameters were then updated by a gradient algorithm to maximize a maximum likelihood function for each parameter. One or several of these parameters were estimated over a planned time segment. Thus, if the segment is very long, a nonlinearity in these parameters over the entire entry can occur. Parameters are used to update the simulator and therefore data is enhanced by flight data.

Use of the RC Circuit Analogy and Time Constant in HEATEST

One method of approximation of the initial temperature T_i is based on an empirically determined RC time constant and on the radiation equilibrium assumption. The circuit analogy is used to compute an equilibrium temperature (T_{eq}) of

$$T_{eq}(t_n) = gT_i(t_n) - (g-1)T_i(t_{n-1}) \quad (17)$$

$$\text{where} \quad g = 1/[1-\exp(-\Delta t/RC)] \quad (18)$$

and the RC time constant value can be equated to the lump parameter

$$RC = Cp\Delta X^2/K \quad (19)$$

This varies with the location in the TPS. In the coating RC is about 1/4 second while empirically RC for the tile is about 3 seconds. The equilibrium temperature works well in the program when you take Q and assume equilibrium. The technique of using the RC analogy is very crude and, when first derived, was not intended for use in flight data correlation. In this report it is being used in HEATEST as an approximate method of obtaining initial conditions, establishing trends, and quick turnarounds.

In this approximation program, conduction effects are approximated by the RC circuit analogy. If the temperature changes, the RC approximation amplifies the heating value but is within reasonable accuracy. The RC approximation amplifies spikes (noise caused by the 8 bit words) and only approximates transients such as angle of attack effects when using $RC=1$. The RC network analogy is explained in Appendix 2.

IV. Flight Test Maneuvers

Objectives

To expand the Orbiter's envelope and remove placards, flight test maneuvers were planned for STS-2 and 4. The AFFTC used a systems approach to the envelope expansion. The placards related to the body flap included heating of the flap and elevons at various Mach numbers and angles of attack, elevator and body flap effectiveness, verification of the basic pitching moment curve (C_{mo}), and lift to drag ratio in the hypersonic regime.

To do this a POPU maneuver from 45 to 35 degrees angle of attack was planned on STS-2 at Mach 20 and three body flap sweeps at Mach 21, 18, and 14. STS-4 planned a PUPU maneuver at Mach 14 and at Mach 8. The flap was cycled through sweeps from 17.1 to 7 degrees positive (downward) deflection.

Performance of Maneuvers on STS-2 and 4.

The entry profiles of STS-2 and 4 occurred as planned. Thermocouple data was recorded on board and telemetry sent in real-time when in view of a station. Unfortunately, critical data was lost on STS-4 when the recorder tailed and real-time data was not acquired until after most of the high Mach heating. Data from the body flap thermocouple used in the data reduction for this report is shown in Fig. 6. The STS-3 and 4 thermocouple data at the same location is also shown for comparison. The elevon schedule for the first four missions has been $\delta_e = -1, 1, 3,$ and 5 degrees respectively with a more

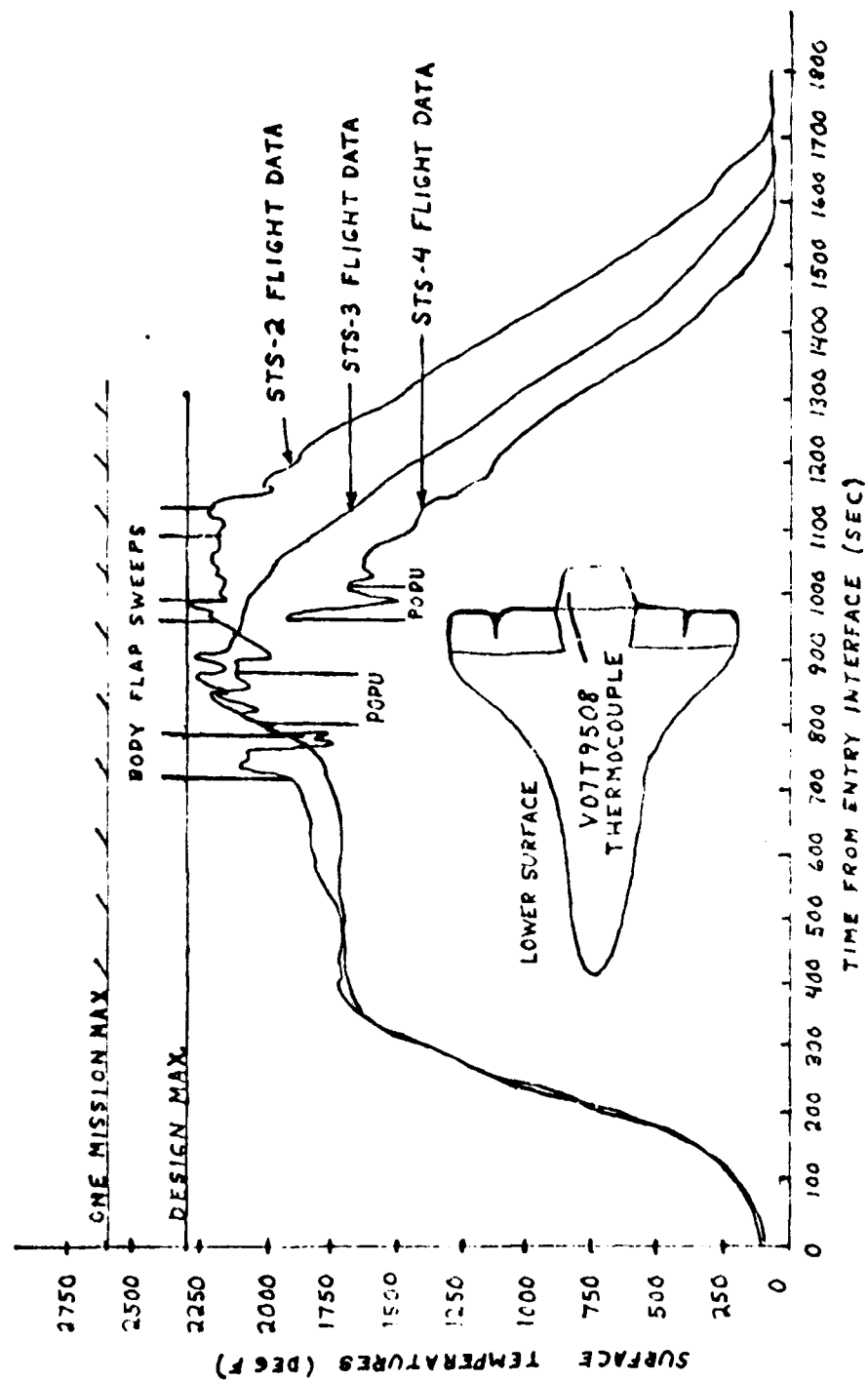


Figure 6. Body Flap Thermocouple Temperature History During STS-2, 3, and 4 Reentries

expanding high Mach number. At the same point the δ_{sr} has been 16, 14, 12, and 4 degrees respectively. Only the STS-2 data is complete enough to do a thorough analysis. The flap and elevon time histories during the STS-2 maneuvers are displayed in Fig. 7. A table of STS-2 maneuver events is shown in Table 1. The heating at the body flap thermocouple location shown indicated a significant increase in temperature over that anticipated. It should be noted that this was not the only location where anticipated thermocouple temperatures varied from actual results. Some locations displayed significantly lower temperatures.

The Orbiter flight control software logic contains a body flap-elevator interconnect which is intended to maintain the elevator on a preplanned schedule as a function of Mach number. On all four test flights it automatically trimmed the body flap at an angle much higher than anticipated. It was concluded that the error was in the basic pitching curve C_{mo} . This information was reduced (Ref 5) to a series of curves as shown in Fig. 8 and 9 comparing the maximum elevon positive deflection (in order to retain its other requirement of entry pitch control) and body flap position for various Mach numbers and angles of attack at nominal and maximum aft CG positions. This data indicates that it is important to know the thermal limitations on the flap and elevons to determine if mission requirements can be met. Other data obtained concluded that the body flap and elevon effectiveness as well as hypersonic lift-to drag ratio were the same as predicted (Ref 5).

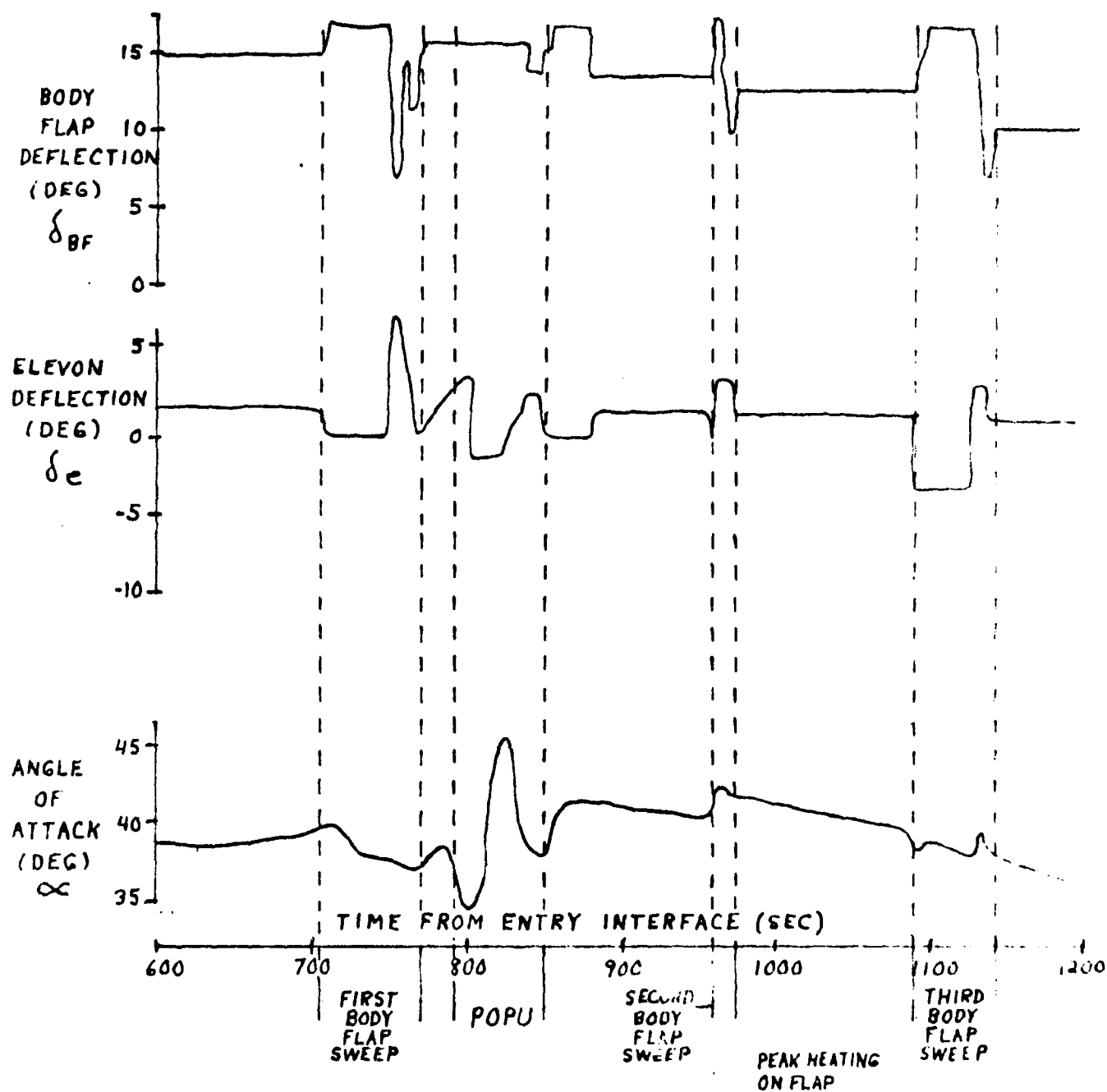


Figure 7. Body Flap, Elevon, and Angle of Attack Variation During STS-2 Flight Test Maneuvers

Table 1 STS-2 Flight Test Maneuver Key Events

EVENT	MISSION TIME (SEC OF GMT)	TIME FROM EI (SEC)	ANGLE OF ATTACK (DEG)	LOG Re	THERMOCOUPLE TEMPERATURE (DEGREES F)
Entry Interface	75037	00.	41.05	2.365	117
1st Flap Sweep (+)	75742	705.	39.86	6.089	1844
Negative Deflection	75786	749.	38.32	6.146	2054
End Sweep	75812	775.	38.12	6.146	1713
POPU (PO)	75830	793.	38.91	6.166	2013
Minimum	75845	808.	34.59	6.178	1992
POPU (PU)	75846	809.	34.59	6.179	1992
Maximum	75865	828.	45.59	6.200	2197
End POPU	75887	850.	38.58	6.220	2065
2nd Flap Sweep (+)	75994	957.	40.21	6.375	2197
Max. + Deflection	75996	959.	39.59	6.38	2228
Negative Deflection	75997	960.	39.60	6.382	2258
Peak Heating	75998	961.	39.40	6.383	2278
Maximum - Deflection	76008	970.	41.41	6.395	2238
End Sweep	76015	978.	41.00	6.401	2126
3rd Flap Sweep	76128	1091.	39.81	6.638	2136
Max. + Deflection	76138	1101.	38.93	6.661	2181
Max. - Deflection	76172	1135.	39.60	6.731	2023
End Sweep	76181	1143.	38.26	6.735	1971

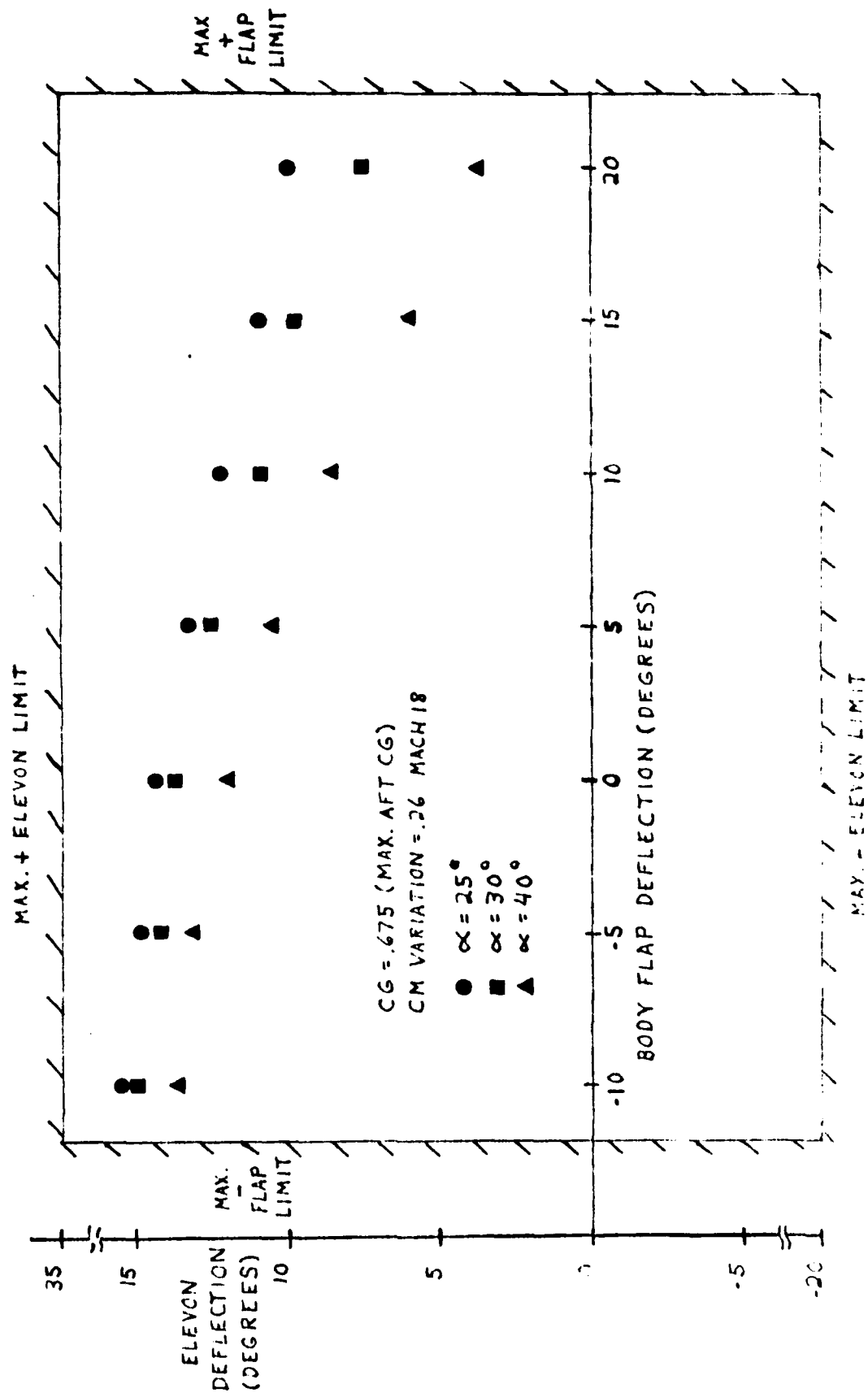


FIGURE 7. Body Flap and Elevon Deflections for Aft Orbiter CG at Mach 18

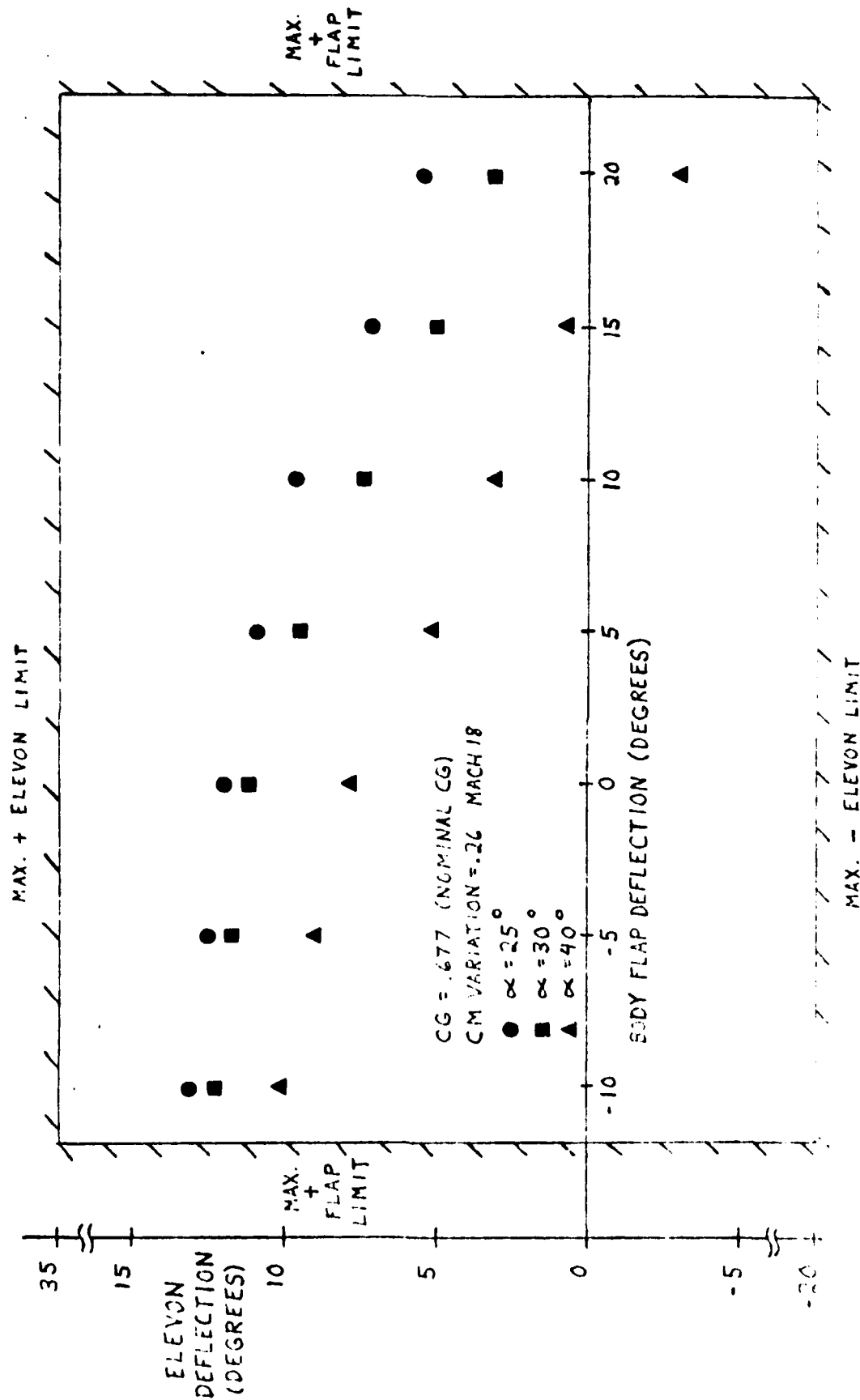


Figure 9. Body Flap and Elevon Deflections for Nominal Orbiter CG at Mach 18

The fixed body flap during the POPU made it possible to identify the Q_∞ and Q_0 using HEATEST if the Q_{Re} derivative is known. Other selected parameters can be expressed to be

$$Q_0, Q_\infty, Q_{\frac{Q_{Re}}{\log Re}}, Q_{\delta_e}, Q_{\delta_{ef}}, X_a \quad (20)$$

where ΔX_a is the effective thermocouple depth or coating thickness. The goal of the data reduction program in HEATEST is to obtain best estimates of these parameters during the maneuver.

V. Results

Initial Computer Runs and Analysis

The STS-2 flight thermocouple data for the location on the body flap shown earlier was input into the HEATEST program. Also input was a Best-Estimated-Trajectory (BET) and atmosphere from NASA Langley Research Center for reducing "model error" caused by bias in the heating ratio from atmospheric density error. A problem of time skews in the data for other points was not apparent in the flight data input at this location. There was however some drop outs of the body flap deflection angle data during one body flap sweep that had been "filled in" prior to its use with this study. Both of the earlier described errors can produce errors in HEATEST estimates which cannot be identified by HEATEST as such. The procedure developed for running the program was to take the entry data and to break up the computer runs into segments. Each segment covered a particular region of the entry where a maneuver was occurring. These segments were further broken down into smaller time segments. For example, a run called HEAT 3 was computed between STS-2 times of 75733 and 75811 seconds GMT, a segment after entry interface (EI) at 400,000 ft. altitude. This is where the first body flap sweep took place. This was further segmented in attempt to have HEATEST estimate individual parameters and uncertainty bounds. These best estimate derivatives or slopes were then used in later time segments to determine if the model would "match" the variations in temperature.

From experience gained by others (Ref 6), derivatives which had the greatest impact were Q , Q_0 , Q_{α} , $Q_{\delta_{ef}}$, and the smallest Q_{δ_e} . The coating thickness (ΔX_a) was initially assumed to be .002 feet and later confirmed. For most runs, the temperature was calculated to obtain an approximate initial condition of the surface temperature using an RC circuit analogy. A best guess of all derivatives at an initial time segment was also made to improve initial conditions. The next segment of time was taken ideally when only one of the heating parameters (α , δ_{ef} , or δ_e) was changing. At this point the program was directed to allow the derivative of the changing parameter to "float" to a new value estimated by the program. This value was then "locked up" or fixed during the next time segment in order to establish the parameter values in that region. As this was taking place the Kalman filter was establishing a new surface temperature based on its updated model parameters. If the parameters were correct, the apriori and aposterori temperatures would match the variations in the flight thermocouple temperature each second within an uncertainty of approximately ten degrees, which is the accuracy of the 8-bit word measurement resolution. Although the δ_e parameter is significant at other Orbiter flap locations near the centerline, its value here is very small and was given a small fixed value during most runs. It was also done in an attempt to prevent trading of its value with other parameters. Otherwise, with the continued variation of the elevon during entry, the Q_{δ_e} would have been required to be "floating" through most of the maneuver times studied.

Using the previous technique was for most cases unsuccessful. The temperatures would drift as more segments were taken within each run and a good match for a long time segment was never truly established. Trading of derivative values such as Q_0 and Q_α or $Q_{\delta_{ef}}$ and Q_α would occur if more than one derivative was being estimated at the same time. Since both parameters may be changing at the same time then both would require estimating. If the values derived from the program were the correct ones the trading may still occur. Examples of the parameter values obtained and there uncertainty bound during different portions of the entry are shown in Fig. 10. The first graph, depicting a search for the right Q_α derivative, were all taken at various portions of the POPU. The second graph depicts a search for the proper $Q_{\delta_{ef}}$ derivative and were all (except the 13 degree run) done during the three body flap sweeps. The third chart again looks for the right Q_α during various portions in the entry. Normally values with large error bounds are not used.

The results of the attempts to calculate angle of attack and body flap deflection effects are not conclusive but those with a small error bound appear to have approximately the same values which may indicate that these are the correct parameter values. Only the trend in the change of these values (if they do change) during the entry may be all that is required to do once HEATEST can be successfully run through the maneuvers.

It was assumed at this point that the problem was caused by one or two items; the Reynold's number derivative and/or a nonlinearity in the other derivatives, or flap flow effects.

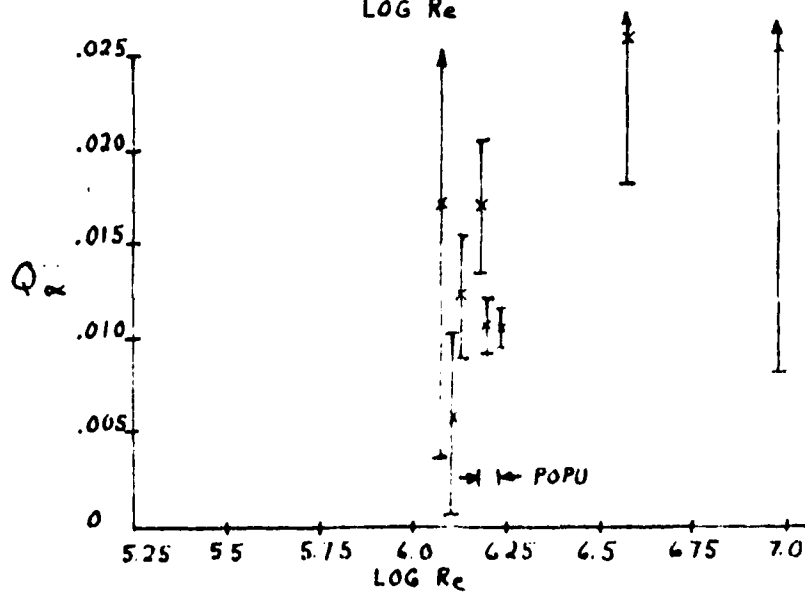
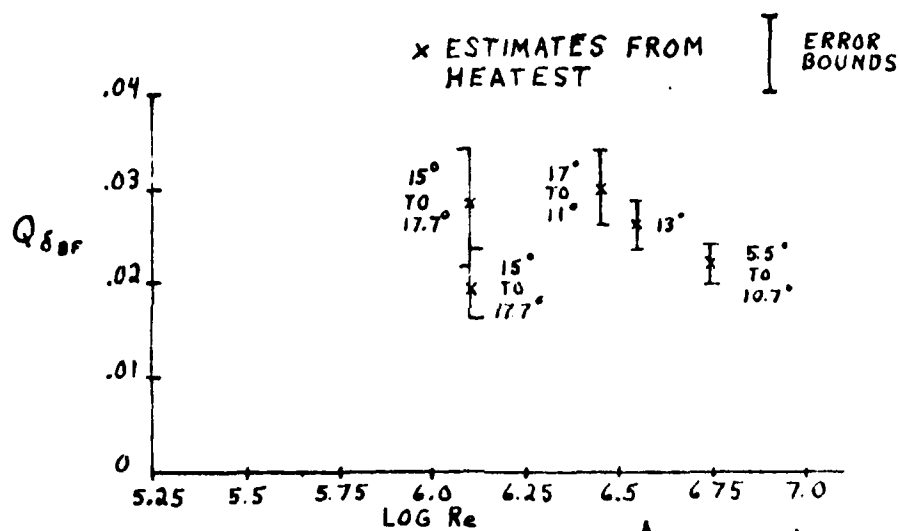
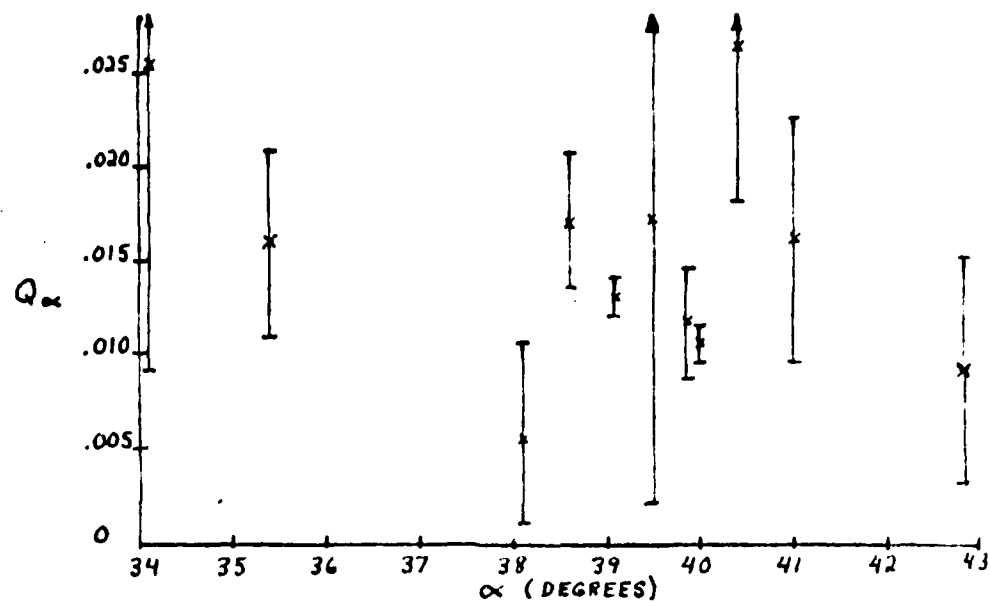


Figure 10. Derivatives and Error Bounds From HEATEST.

The Reynold's number derivative is unique in that flow transition causes a rapid increase in its generally small value and then decreases rapidly when fully turbulent. This effect can also cause difficulty in interpreting the results if the transition occurs during the maneuver. If interpreted correctly it indicates sensitivity to transition in one of the variables, particularly if the flow returns to a laminar state. Such a condition occurred on STS-4 on the lower surface centerline. The assumed Reynold's number effect could also be a Mach number effect and real gas effect but the two cannot be separated during a given flight other than by theory. The Mach number effect could also be pulled out in lieu of Re . The Reynold's number changes so slowly that the only way to accurately determine its value is to run the program for as long as possible (over 100 seconds is best) with no other changes taking place in the region. Unfortunately, the region in question is very dynamic and the program as established could not distinguish Reynold's number, Q_0 , and Q_∞ effects so the slope could not be obtained. When the Reynold's number runs were made these too would not converge except at one point in the entry. This single point was not sufficient to establish a trend. Figure 11 depicts the $Q_{LOG Re}$ verse $LOG Re$ results obtained. Although the error bounds appear small it must be remembered that derivatives are trading values resulting in a small error band for an incorrect value.

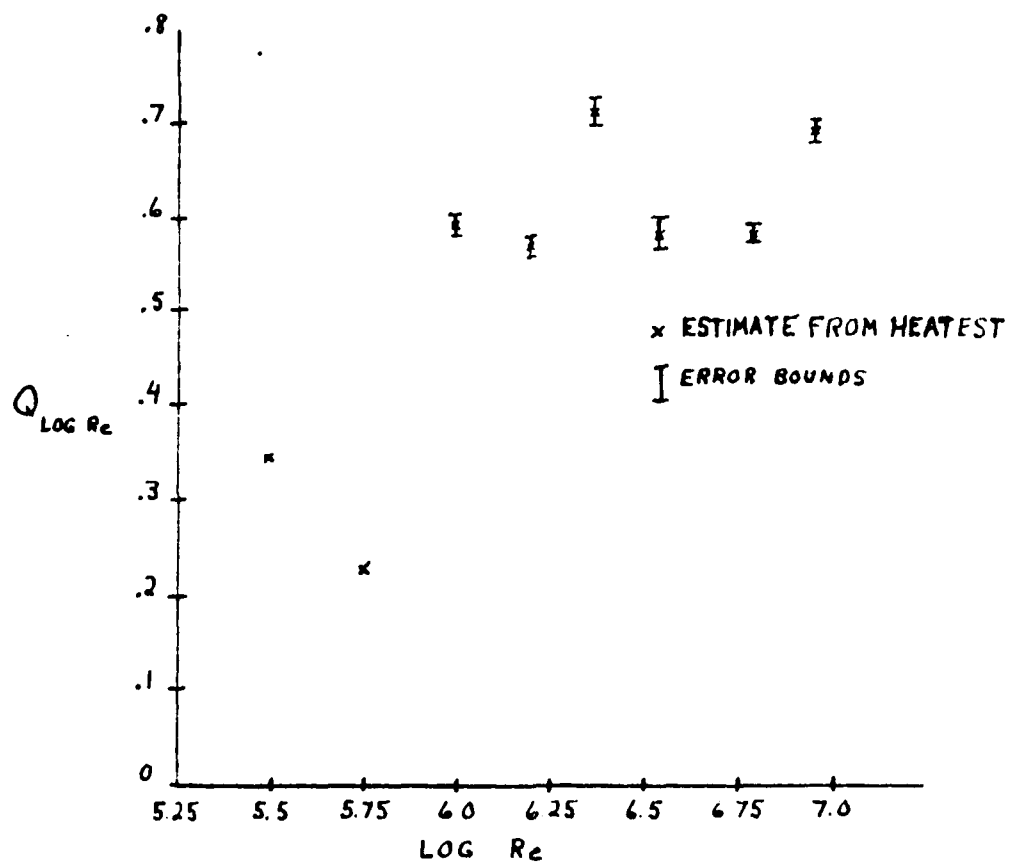


Figure 11. Q Versus LOG Re

Comparison of Heating Models

Two methods of removing nonlinearity effects are to change time segments in HEATEST or change the model. Many time segments were tested without success. In systems identification theory model error is a major concern and problem (Ref 1). Since the model had worked with very little difficulty in other Orbiter regions it was surprising and disturbing that it occurred at this point. The only option at this point was to investigate other more complex models based on more complex theories and compare them. In comparing these theories it was not the intent to say they were totally accurate and therefore could be used in predicting. The main objective was to use various theories to see if they agree with the flight data in magnitude, slope, or linearity.

In first plotting the flight condition Q/Q_{ref} versus $\log Re$, obtained by only estimating Q_0 in HEATEST with assumed value of Q_∞ and Q_{ref} , the Reynold's analogy theory was compared for laminar and turbulent flow. This is shown in Fig. 12. Hand calculations revealed that the turbulent flow more closely matched the flight data. Since the theory in the turbulent case uses $Re^{.8}$ an axis change of Q/Q_{ref} verse $Re^{.8}$ revealed a more linear slope. Calculations of these results and others are in Appendix A.

Calculations using the normal shock tables and Reynold's Analogy as Rockwell established in their data book (Ref 7) were also compared. These values did not match in magnitude or slope. In the region of interest, the magnitude was too high at the start and too low at the end.

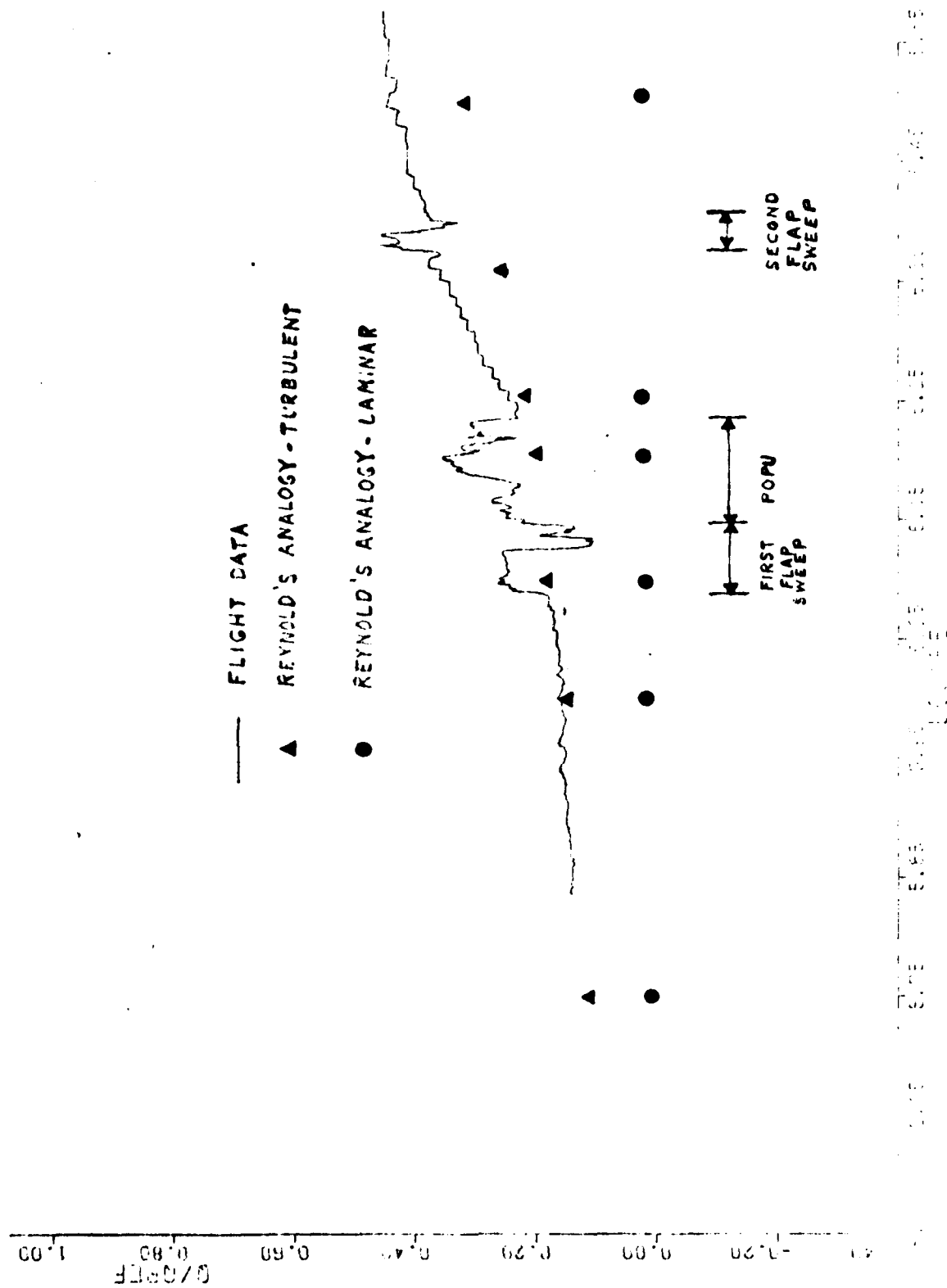


Figure 12. Q/QREF versus X/B for Flight Data and Reynold's Analogy

In another approach, it is considered we empirically know that down the centerline of the Orbiter prior to the boattail expansion that the flow is approximately Mach 3 (Ref 6). The stagnation and after the shock temperatures can be evaluated. From these values, the conditions at the flap and more accurate values of viscosity, Reynold's number, and Q/Q_{ref} can be calculated. The flap angle can be fixed verses changes in time and $Re^{.8}$. At a given $Re^{.8}$ the flap can be changed in deflection angle and Q/Q_{ref} changes due to this deflection can be determined. The minor changes in the angle of attack are assumed to be linear and the elevon changes are not significant at this point on the flap. The calculated results again did not match in slope but were close to the flight data in magnitude.

It was stated in a recent AIAA paper (Ref 8) that Newtonian flow analysis could be used for the lower surface of the Orbiter in this hypersonic regime. Calculations using this approach concentrated on determining the specific heat at high Mach numbers (Ref 9) and low density. The flap angle, weak shock expansion, and shock tables determined the downstream Mach number, density, velocity, Reynold's number, and viscosity. When calculating from these values, Q/Q_{ref} for $Re^{.8}$ values were not close in slope to the flight data. However, the magnitude of values was close to the flight results. It was observed, in this analysis and the previous weak shock calculations, that variations in body flap at a given Mach number and angle of attack did not change significantly the Q/Q_{ref} values. The Newtonian analysis however revealed that

the changes in angle of attack did significantly influence the slope of the Q/Q_{ref} values.

A fifth approach was to consider the Eckert flat plate formulas (Ref 10) used in the program to calculate the heating ratio Q/Q_{ref} but now adding the downstream conditions and the deflection angle terms. Using the turbulent flow equation and plotting the resulting Q/Q_{ref} values verses $Re^{.8}$ for the same entry conditions as previous calculations resulted in a series of points slightly higher than the flight data at the beginning, crossing the flight values during the first body flap sweep and POPU maneuvers, then leveling off at values below the flight data later in the entry.

The sixth approach was to consider another model that would use the approximate downstream conditions in calculating the heat rate and remove the influence of Reynold's number completely from the problem. By knowing that the Q value in the Newtonian and Reynold's analogy is a function of Stanton number and enthalpy, as well as the Reynold's number and distance from the stagnation point, the Q_{ref} equation can be rearranged to be a function only of the downstream density, velocity, and enthalpy with the distance and Stanton number a constant (Ref 11). Enthalpy could be and was calculated using the freestream velocity or the specific heat and stagnation temperature for the input conditions used previously. The results were encouraging. Compared with the earlier approaches and flight data, the results followed in close agreement with the flight data through the first two maneuvers and its magnitude matched the flight data Q/Q_{ref} at the latter

body flap sweep. It must be remembered that the flap deflection for these calculations is considered constant and therefore no body flap sweeps are input into the calculations.

The seventh and final method to be examined was an approach used by NASA in their analysis of the heating, the Spalding and Chi technique (Ref 12). This method finds the value of the skin friction coefficient, C_f . To use this technique, the flap conditions were assumed to be as they were in the weak shock calculations. Assuming that the flap prior to the weak shock experiences a free stream Mach number of 3, the edge condition experienced by the flap becomes $M_2=1.27$ for a flap deflection of +7 degrees. The procedure described in the reference was performed for the seven entry points previously used. The result was an almost linear reduction of the C_f value from .99 to .80 from that of the approximation of .006 used in the Stanton number-Enthalpy calculations. When this value was applied to those calculations, the resulting Q/Q_{ref} magnitude was almost identical to the flight data before, during, and through the POPU maneuver. However, because the flap deflections were not considered, the resulting values did not reflect a change during the two body flap sweeps.

Figure 13 graphically compares all of these methods. The Reynold's analogy, Eckert, and Enthalpy-Stanton number values with and without the Spalding and Chi C_f values are more closely compared with the flight data in Fig. 14. Figure 15 displays the wind tunnel data, the NASA simplified heating model and the weak shock results using $M_\infty=3$ prior to the flap

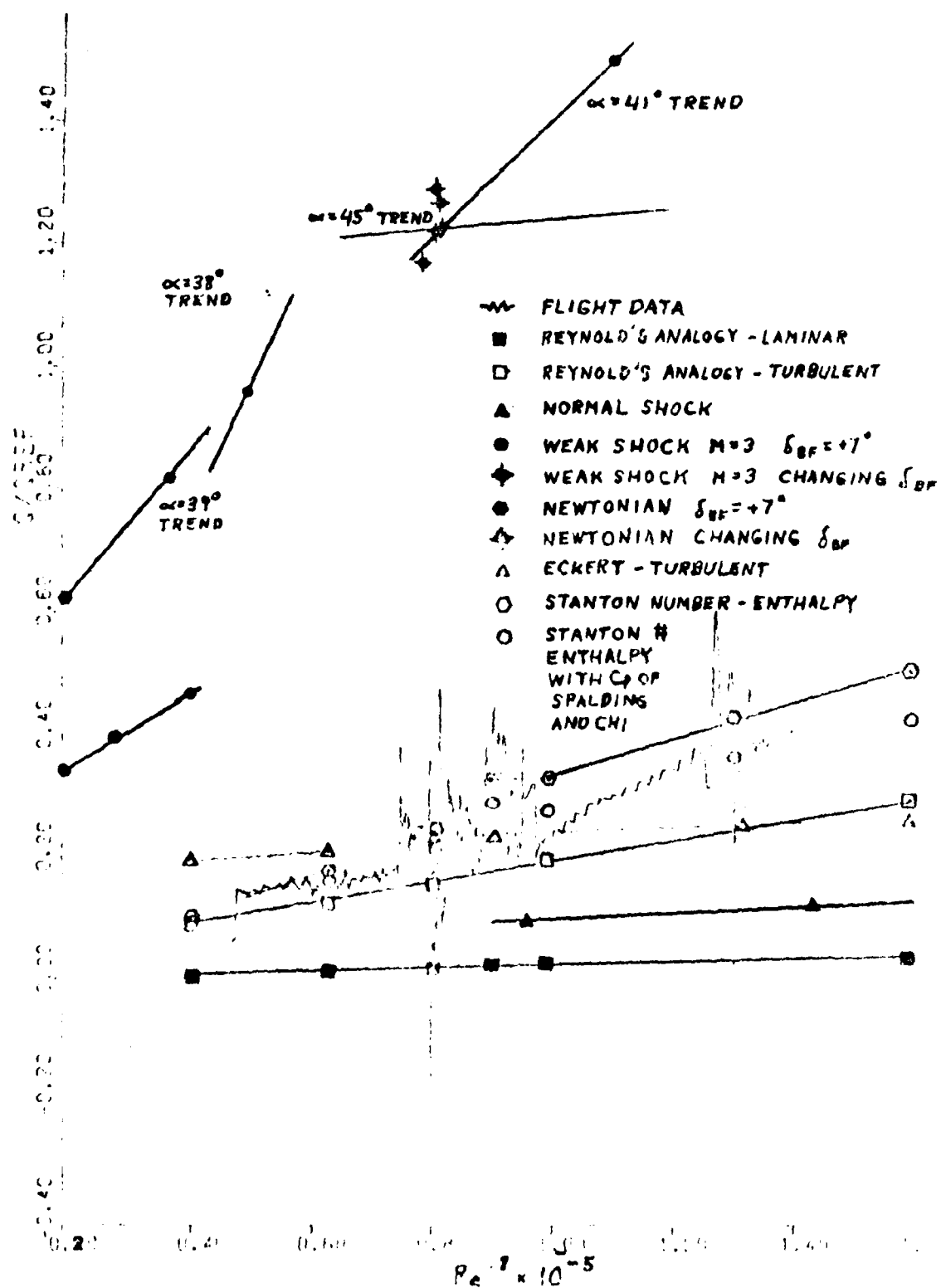


Figure 13. Q/Q_{ref} Verses $Re^{1/2}$ For Flight Data and Calculated Heating Models

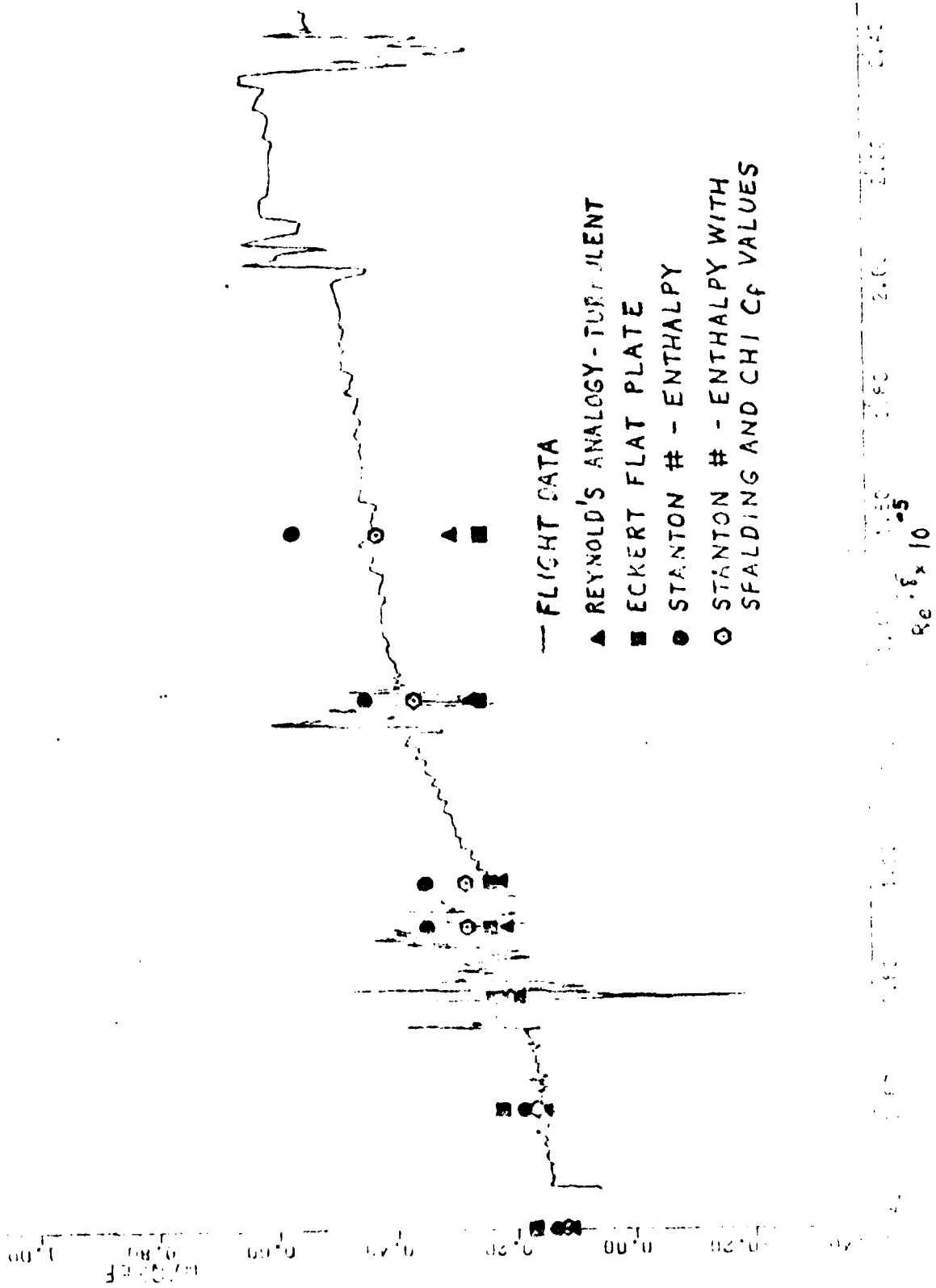


Figure 17. Reynold's Analogy, Eckert, Stanton Number-Enthalpy, and Flight Data Q/Q_{ref} Verses $Re^{.8}$

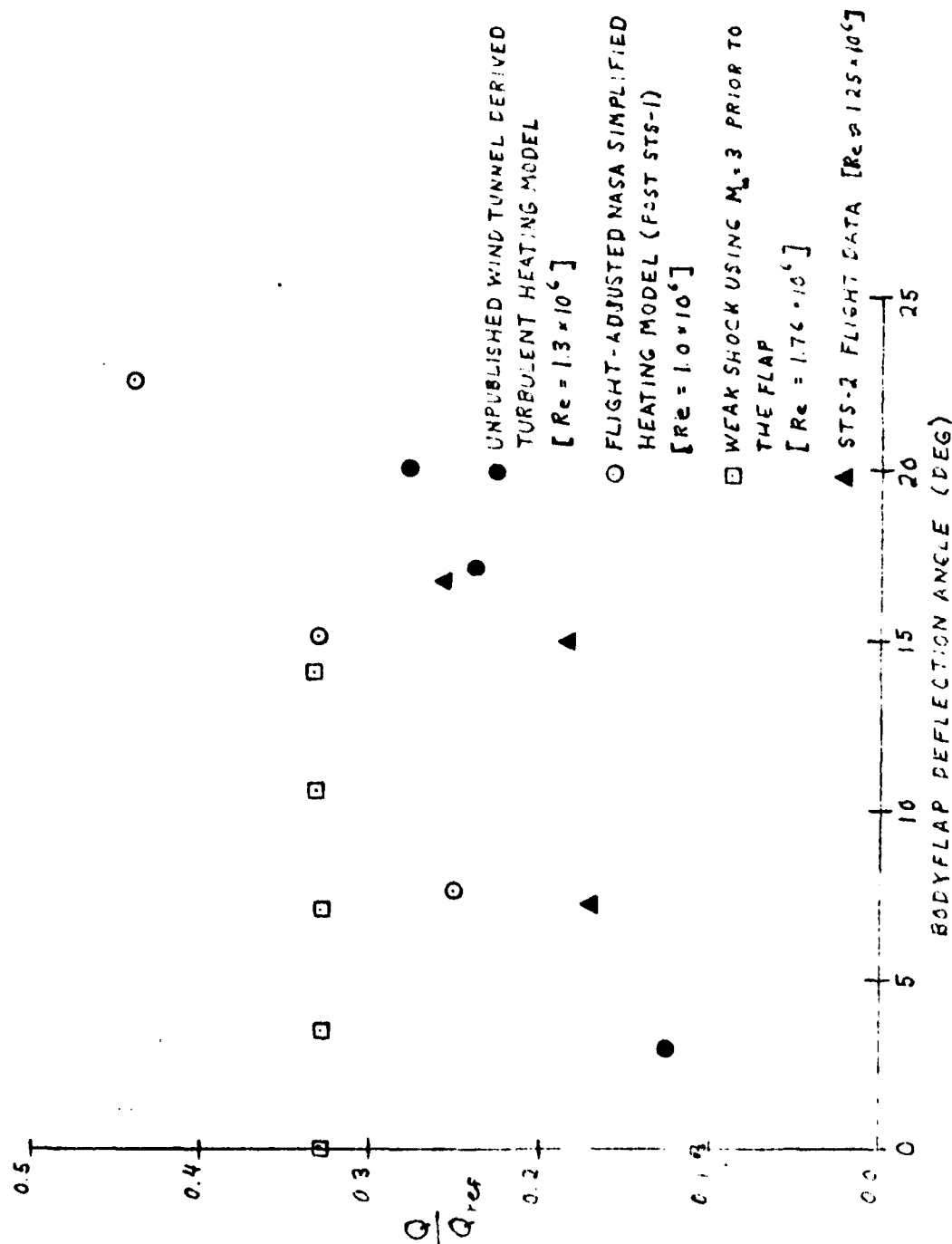


FIGURE 10. HEAT FLUX, NASA, AND WEAK SHOCK MODELS AND FLIGHT DATA Q/Q_{ref} VERSUS BODY FLAP DEFLECTION

The Enthalpy-Stanton number approximation combined with the Spalding and Chi Cf values appears to be closest to the flight data but would be extremely difficult to use in the HEATEST program. The primary difficulty is in determining the downstream conditions accurately at the flap. This is also true of the other approaches attempted except for the Reynold's analogy and the Eckert equation not using the deflection correction factor and the temperature ratio T^*/T_0 . It is obvious that the weak shock and Newtonian flow analysis have a similar problem. Placing the new Cf values in the Newtonian and Weak shock calculations made no significant change in their lack of accuracy compared to the flight data. Invalid assumptions made or calculations performed altered the downstream Reynold's number in the weak shock calculations and the magnitude of the Q/Q_{ref} in the Newtonian analysis.

In the calculations for the downstream conditions several assumptions must be made. First, that the freestream flow past the expansion at the boattail reaching the flap is approximately Mach 3. Second, that the flow is not detached or reattaching prior to reaching the flap; an assumption in question when flow is analyzed in photos at these Mach numbers. Third, that the flow condition at the point and times in question are all in one state, turbulent flow. The flow may transition back and forth depending on the entry conditions such as angle of attack, deflection angle, and Reynold's number. All these factors complicated the analysis while simultaneously it is being attempted to use a single model in HEATEST to determine the resultant heating.

In using the Stanton Number-Enthalpy analysis in eliminating dependence on Reynold's number it produces the equation

$$Q = St / \rho V_e H_s = St (\rho_\infty V_\infty^2 / 2) ((\rho_2 / \rho_\infty) * (V_2 / V_\infty)) \quad (21)$$

where ρ_2 and V_2 are the downstream density and velocity and ρ_∞ and V_∞ are the freestream density and velocity. Assuming that the Stanton number changes are insignificant, this produces

$$(\rho_2 V_2 / \rho_\infty V_\infty) = f(\alpha + \delta_{gr}) \quad (22)$$

and therefore

$$Q = St \rho_\infty (V_\infty^3 / 2) f(\alpha, \delta_{gr}) \quad (23)$$

or rearranging

$$Q / St \rho_\infty (V_\infty^3 / 2) = f(\alpha, \delta_{gr}) = Q / Q_{ref} \quad (24)$$

where the new Q_{ref} could be

$$Q_{ref} = St \rho_\infty (V_\infty^3 / 2) = (Cf / 2) \rho_\infty (V_\infty^3 / 2) \quad (25)$$

Using Spalding and Chi conditions, St and Cf are fixed at a given reference value (α_0). The \tilde{Q} to put into the HEATEST program could now be this new \tilde{Q} generated by this method so

$$\tilde{Q} = f(\alpha, \delta_{gr}) = f_0 + f_\alpha(\alpha - \alpha_0) + f_{\delta_{gr}}(\delta_{gr} - \delta_{gr_0}) \quad (26)$$

$$\text{or} \quad Q = Q_0 + Q_\alpha(\alpha - \alpha_0) + \tilde{Q}_{\delta_{gr}}(\delta_{gr} - \delta_{gr_0}) \quad (27)$$

our basic HEATEST equation. The difficulty is we really can't know the $M_\infty = 3$ flow conditions prior to the flap so we can't

using the freestream conditions which may not be the same. However, it was demonstrated earlier at least for the region of interest these conditions combined with this method produce good results.

Input of Models into HEATEST

Returning to the reason for running these models, the HEATEST program took the heat rate as

$$\bar{Q} = Q/Q_{ref} = \bar{Q}_0 + \text{Ref}(1) + \bar{Q}_\alpha (\alpha - \alpha_0) + \bar{Q}_{\log Re} (\log Re - \log Re_0) + \bar{Q}_{\delta_{eff}} (\delta_{eff} - \delta_{eff_0}) \quad (28)$$

where the program uses Q_{ref} as the stagnation condition and $\text{Ref}(1)$ is zero. It was assumed the Q_{δ_e} derivative was insignificant. At the point in the entry where the flight test maneuvers took place, HEATEST was repeatedly run in an attempt to find Q_α and $Q_{\delta_{eff}}$ by taking $Q_{\log Re}$ that was assumed to correspond to that and Reynold's number. When the Q_α and $Q_{\delta_{eff}}$ derivatives and Q_0 magnitude could not converge on a value for any length of time, the $Q_{\log Re}$ derivative was attempted to be found over a long time period only to discover the slope of this derivative was not linear. So the approach was taken to try to eliminate or minimize the Q_{Re} effect. This is one of the three derivatives varying with time, the others being Q_α and Q_α . By eliminating these two by subtracting, the other can be determined since it is assumed to be only a function of α , δ_{eff} , and Reynold's number. The conditions required to do this relate to the magnitude, slope, and correct functional variation (linear effects) of the flight data results. When

this Reynold's number effect is established, models in the HEATEST can be modified and then other heating derivatives estimated during the maneuvers. It is desired then to place the Q_{Re} derivative back into the program as a functional variation that would make it linear, a heating reference variable such as \bar{Q} Eckert that could make it linear, or a reference value that would completely eliminate the Reynold's number derivative such as in equation (25).

By assuming we know \bar{Q}_0 , \bar{Q}_α , and $\bar{Q}_{\delta_{gr}}$, then the derivatives can be found by solving (when using $Re^{\frac{1}{4}}$)

$$Re^{\frac{1}{4}} Q_{Re} (Re^{\frac{1}{4}} - Re_0^{\frac{1}{4}}) = \bar{Q} - \bar{Q}_0 - \bar{Q}_\alpha (\alpha - \alpha_0) - \bar{Q}_{\delta_{gr}} (\delta_{gr} - \delta_{gr_0}) \quad (29)$$

The program can evaluate \bar{Q} using any reference we wish. When this is plotted verses a Re number that produces a linear slope the result should be a nearly straight line with some bias or magnitude. A ΔQ which equals

$$\Delta \bar{Q} = \bar{Q} - \bar{Q}_0 (\alpha - \alpha_0) - \bar{Q}_{\delta_{gr}} (\delta_{gr} - \delta_{gr_0}) = (\bar{Q}_0 + Re \text{ term}) \quad (30)$$

it now placed in the HEATEST program for numerous sequential time segments of approximately five seconds duration each and, assuming that the $Re^{\frac{1}{4}}$ term was zero, results in an upward sloping line representing the \bar{Q}_0 magnitude and the Re term for a specific reference α_0 and δ_{gr_0} . Thus the α and δ_{gr} have been removed leaving the Re effect and some \bar{Q}_0 magnitude. The computer always obtains the \bar{Q}_0 magnitude and is not a problem except in very extreme cases when a new model should be considered. If the right reference is used the model can be used in

be determined the result would be a straight line of zero slope parallel with the Re number axis (the effect eliminated) with a constant magnitude of \bar{Q}_0 . If the magnitude \bar{Q}_0 were also subtracted out, the line would be at zero. This result is our goal, accomplished by changing the X axis Re number value. If the slope is not zero but reduces the slope of the Reynold's number effect, then it is still helpful in our analysis because it can then be assumed that \bar{Q}_{Re} is essentially constant over the short time segment in the entry where a maneuver is executed. All of those results assume that you have the correct \bar{Q}_∞ and $\bar{Q}_{f,r}$ to subtract out. \bar{Q}_∞ and $\bar{Q}_{f,r}$ may be input as functions of Re when maneuvers are available at various Mach numbers. If the "perfect" model is found the \bar{Q}_{Re} may be eliminated.

From the previous analysis of the models, the ones showing the most promise to be used in this approach were the Stanton Number-Enthalpy results using Spalding and Chi and the Eckert flat plate model for turbulent flow. However, the technique was first used to observe if the Q/Q_{ref} stagnation model could be used. As a first attempt at analyzing the derivatives and there effects on the slope of this heating model, the RC circuit analogy was used for plotting Q/Q_{ref} stagnation verses $Re^{-1/4}$. The result of "turning on" the derivatives it was hoped would result in each removing the heating effects they create and remove the slopes of their derivative in the model. If all the derivatives input into the model were correct, the result using the RC approximation would produce a new ΔQ which would be a linear function.

Figure 16 displays the ΔQ stagnation verses $Re^{.8}$ using the RC approximation. The result indicates that the slope of the line with all derivatives input (showing heating effects from no sources) changes at least once. This line is compared to the line generated from the heating model reference with the derivative $Q_{\delta_{bf}}$ removed to include body flap effects. As the comparison indicates, during the first and second flap sweep the flap effect is significantly reduced but not totally. Also evident is that the slope during the third sweep changes in the opposite direction. This indicates that the flap derivative removed may be too high. The lower magnitude of the heating in the line produced with $Q_{\delta_{bf}}$ is due to the change in the body flap position between the $Re^{.8}$ of .55E5 and 1.2E5 from 14.9 to 13.3. Likewise, if the Q derivative were removed here, the α being slightly higher (excluding the maneuvers) would produce a shift in the magnitude positively.

The Eckert model was studied in a similar approach for comparison. Figure 17 compares the ΔQ Eckert verses Re with no heating effects and with the $Q_{\delta_{bf}}$ derivative removed. The discontinuity is more apparent in this case. The body flap derivative removes most of the flap effects and changes the slope of the function in the same manner as it did in the stagnation model.

The use of the RC analogy produces noisy and possibly inaccurate results. To be sure the model can or cannot be used in HEATEST, the stagnation and Eckert models were placed into the program with and without the T^* correction factor. The purpose in this was to see if the Q/Q_{ref} Eckert is better

ASY
FLAP
SPEED
FOPU

INPUT PARAMETERS AND CONDITIONS
 $Q_0 = .5891$
 $Q_A = .0533$ AT $\alpha = 38.12^\circ$
 $Q_{0,6F} = .0793$ AT $\delta_{8F} = +14.5^\circ$

ΔQ
 STAGNATION
 WASHING EFFECTS

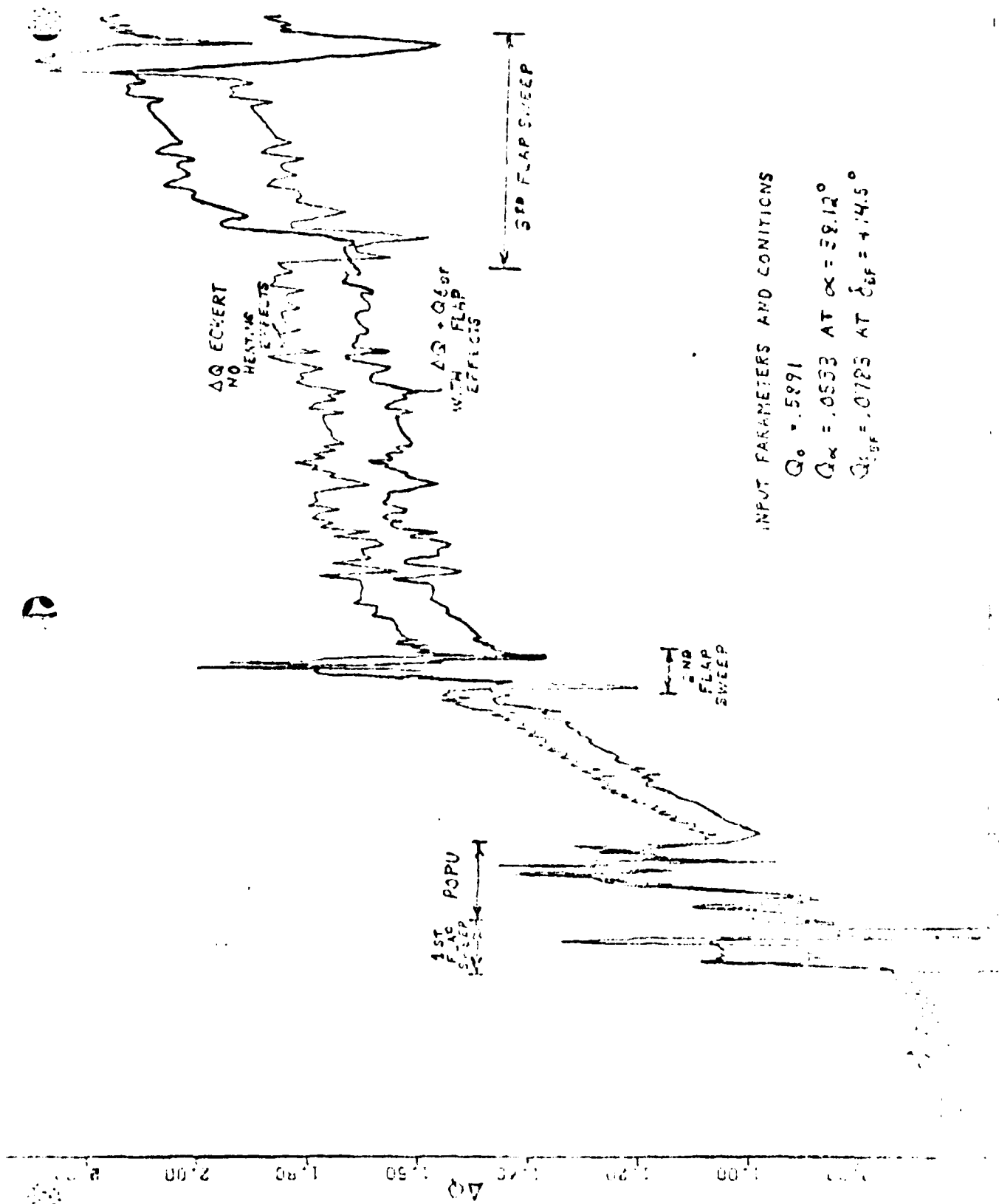
$\Delta Q = Q_{0,6F}$
 WITH
 FLAP
 EFFECTS

THIRD FLAP SLEEP

SECOND
 FLAP SLEEP

10^{-5}

FIGURE 16. ΔQ STAGNATION WASHING EFFECTS IN FLAP USING FC APPROXIMATION



INPUT PARAMETERS AND CONDITIONS

$$Q_0 = .5891$$

$$Q_\alpha = .0533 \text{ AT } \alpha = 38.12^\circ$$

$$Q_{\delta_{LF}} = .0725 \text{ AT } \delta_{LF} = 4.14.5^\circ$$

Figure 17. ΔQ - eject volumes Re^8 using PC Approximation

If it was, it could be put back in to HEATEST as a variable as described earlier. To input this into HEATEST the initial conditions were established at the start of the $Re^{\frac{1}{2}}$ value of interest. HEATEST was allowed to run for increments of five seconds each generating a Q/Q_{ref} Eckert value for each segment. This was done to eliminate noise and generate a slope from the combination of five second "steps". The plot of this run and a similar one done for Q/Q_{ref} stagnation are shown together in Fig. 18. The results indicate again that the Eckert has a larger magnitude and slope compared to the stagnation model. Time did not permit the insertion of the heating derivatives to confirm the preliminary conclusions drawn from the RC analogy.

Time did not permit the input of the Stanton Number-Enthalpy model with the Spalding and Chi Cf values into HEATEST. If it were used, the same Q/Q_{ref} for its model would have been performed. If the results confirm the calculations performed, this model for Q/Q_{ref} , when calculated verses $Re^{\frac{1}{2}}$ would produce a curve that would eliminate \bar{Q}_{∞} effects and possibly \bar{Q}_{∞} effects. Thus the flight data would match the model for the maneuvers with the exception of changes in body flap. If they were held fixed, then the model most likely would produce an upward sloping curve. This curve could be similar in appearance to the models shown in Fig. 18 although calculations indicate it would be much more linear. The curve would essentially be for a constant

$$\Delta Q = \bar{Q} - Q_{\infty}(\alpha - \alpha_0)$$

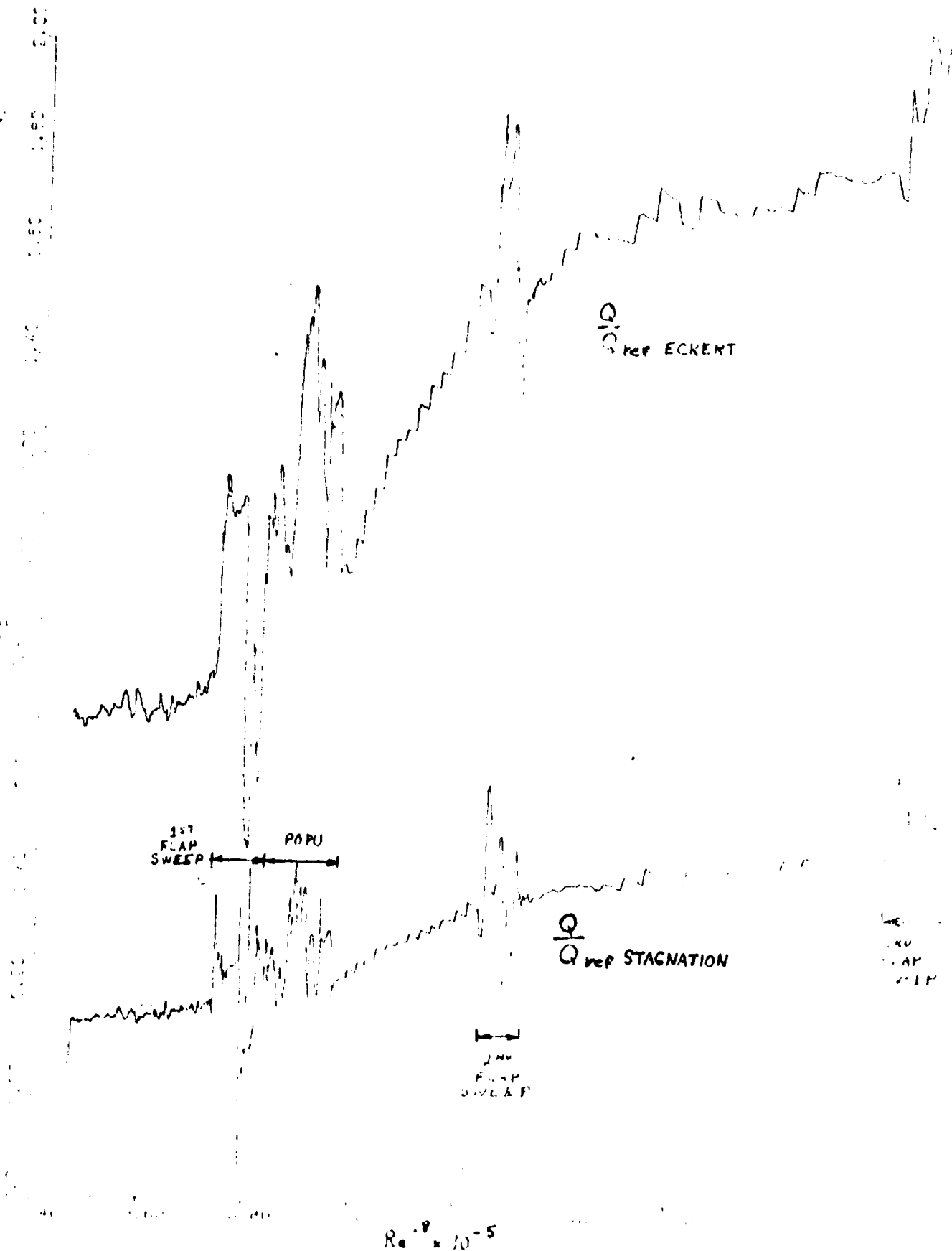


Figure 18. Q/Q_{ref} Stagnation and Eckert in $Re^{0.5}$

From ΔQ , a δ_{BF} value can be input to produce the function

$$\bar{Q} = Q/Q_{ref} \Big|_{\substack{\alpha=\alpha_o \\ \delta=\delta_o}} = \bar{Q}_\alpha (\alpha - \alpha_o) - \bar{Q}_{\delta_{BF}} (\delta_{BF} - \delta_{BF_o}) \quad (32)$$

From the above equation the derivatives \bar{Q}_{BF} , \bar{Q}_α and the magnitude \bar{Q}_o would all be established and, if done correctly, should produce a "match" with the flight data. This then would be the new process of determining the heating rate derivatives for the body flap from HEATEST.

VII. Conclusions

An attempt to use the HEATEST program in its original form failed to properly determine all the heating derivatives that effect the body flap. The angle of attack and body flap deflection effects were approximated but definitive values could not be verified due to the problems in calculating the Reynold's number effect. The Reynold's number effect was found to be nonlinear. A scientific approach was used to determine if a model could be found that would linearize or eliminate the Re effect. Several techniques were studied and at least one was found that could be applied to HEATEST. The indications are that the point studied on the flap was in turbulent flow but the possibility still exists that it could have been in transition or a local flow reattachment.

The question still exists as to how this approach can be used on the centerline body flap thermocouple point which appears to be affected much more by elevon deflection than the one studied. The analysis done in this report is only the first step in studying the overall heating effects in this area. It is a critical point in later missions and its determination is vital prior to the high cross-range missions in the future.

Recommendations

The Spalding and Chi technique incorporates many assumptions but if used at a reference and condition could be used as a valid Qref model in HEATEST. I recommend that an attempt be made to incorporate the Enthalpy-Stanton number relationship using the Spalding and Chi Cf values. This appears to be the most accurate means of determining the heating effects during the maneuvers.

If the Spalding and Chi technique cannot be used, I recommend attempting to use the Eckert turbulent flow equation or attempt to use models where Reynold's number is not used.

The HEATEST program presently uses the Kalman filter to take the equation

$$X(t) = Fx(t) + GU(t) \quad (33)$$

and produces the new equation after the time increment

$$X(t+\Delta t) = Fx(t) + GU(t) \quad (34)$$

The function $Fx(t)$ has the value

$$Fx(t) = e^{At} \quad (35)$$

This function could be left alone after the first iteration and save computer time. However, in a related thesis a student has taken advantage of the A matrix being triangular and has substantially reduced the computer time.

I recommend that as a means of determining the Reynolds number that HEATEST should incorporate all available Test Maneuver data from STS-2, 3, and later missions when

specific time interval where the same conditions occur in the entry and the derivatives compared to obtain a more accurate value of \bar{Q}_{re} .

I recommend a possible change in the flight test maneuver philosophy by going to shorter maneuvers where Reynold's number is not a problem. Another approach may be to do the opposite by trying a series of maneuvers sequenced out to get slopes and derivatives of other parameters leaving the Reynold's number effect to be established last.

Due to the fact that there was so much difficulty in modeling the entry heating at the body flap it is apparent that one or several things are taking place that I am not aware of. Based on my analysis, I would recommend that priority emphasis be placed in determining what is happening here. More flight test maneuvers should be performed for analysis. There should be maintained a means of obtaining thermocouple data from these and other body flap locations on future flights. A mission with a landing at Kennedy Space Center or using properly located ARIA aircraft would allow thermocouple data to be sent in real-time during the entry (assuming little if no blackout takes place) removing the need for the recording and post flight playback on the orbiter (which has been unsuccessful in several previous attempts). Until the heating can be reliably predicted in this area, I also recommend that no WTR missions be performed where a high angle of attack and maximum aft CG condition takes place producing possible excessive heating.

Bibliography

1. Hodge, J. K. and Audley, D.K. "Aerodynamic Flight Envelope Expansion For A Manned Lifting Reentry Vehicle (Space Shuttle)", AGARD Paper 3A. AGARD Flight Mechanics Panel Symposium, October 1982.
2. Maybeck, P. S., Stochastic Models, Estimation and Control, Academic Press, 1979.
3. "Test Results From the NASA/Rockwell International Space Shuttle Heating Test (1979). Conducted in AEDC-VKF Tunnel B", AEDC-DR-75-17, February 1975.
4. Hodge, J. K., and Phillips, P. W., "Flight Testing a Manned Lifting Reentry Vehicle (Space Shuttle) for Aerothermodynamic Performance", Paper AIAA-81-2421 AIAA/SETP/SPTE/SAE/ITEA/IEEE 1st Flight Testing Conference, November 1981.
5. Kirsten, P. W., and Richardson, D. R., "Predicted and Flight Test Results of the Performance and Stability and Control of the Space Shuttle From Reentry to Landing", AGARD Paper 3H. AGARD Flight Mechanics Symposium Panel, October 1982.
6. Hodge, J. K., Personal Communication, AFETC, 1981.
7. Space Shuttle Orbiter Entry Aerodynamic Heating Data Book, Rockwell International Space Division, Document Number SB73-SH-0184 C Revision, Books 1 and 2, October 1978.
8. Rakick, J. V., and Stewart, D. A., "Results of a Flight Experiment on the Catalytic Efficiency of the Space Shuttle Heat Shield", AIAA Paper 82-0942 AIAA/ASME 3rd Joint Thermophysics, Plasma, and Heat Transfer Conference, June 1982.
9. Cox, R. N. and Crabtree, L. F. Elements of Hypersonic Aerodynamics, English University Press, 1968.
10. Eckert, E. R. G. "Survey of Boundary Layer Heat Transfer at High Velocities and High Temperatures", WADC Technical Report 59-610, WADC, April 1960.
11. Hankey, W. L., Neumann, R. F., and Flierl, R. H. "Design Procedures For Computing Aerodynamic Heating At Hypersonic Speeds", WADC Technical Report 59-616, WADC, June 1960.

12. Spalding, D. B. and Chi, S. W. "The Drag of a Compressible Turbulent Boundary Layer on a Smooth Flat Plate With and Without Heat Transfer", Journal of Fluid Mechanics, Vol. 18, Part 1, Jan. 1964, 117-143.
13. "Equations, Tables, and Charts For Compressible Flow, NACA Report 1135, 1953, GPO.

Appendix A

Derivation of Heating Model Solutions

To perform the following calculations reference points were chosen at various times during the point in the entry when flight test maneuvers were being performed on STS-2. In order to do the calculations the body flap had to be assumed fixed during these times and a second set of calculations performed at one time in the entry with the flap being deflected. The table of these reference points is shown in Table 2.

Procedure for Calculations Using Reynold's Analogy

Using Reynold's Analogy

$$Cf/2 = A/Re^N \quad (1)$$

$$St = Cf/2 = Nu/RePr \quad (2)$$

$$Q = h(Taw - Tw) \quad (3)$$

$$Nu = hL/K \quad (4)$$

Substituting (3) into (4)

$$Nu = QL/K(Taw - Tw) \quad (5)$$

Substituting (2) into (1)

$$Nu/RePr = A/Re^N \quad (6)$$

Substituting (5) into (6) and rearranging

Table 2. Entry Reference Conditions
For Heating Method Calculations

Ref Pt	V_{∞} ft/sec	Mach #	ρ E-7 slugs/ft	Log Re	Re E6	T deg R	α deg s	Qref
1	24178	26.1	.59	5.75	.56	356.7	39.11	60.8
2	22605	24.2	1.15	6.00	1.00	364.2	39.31	67.4
3	20985	21.8	1.74	6.125	1.33	386.9	38.08	65.0
4	19977	20.1	2.29	6.20	1.59	412.2	44.66	63.5
5	18804	18.6	2.80	6.25	1.78	425.8	41.51	57.6
6	17203	16.5	4.50	6.39	2.46	446.5	40.89	54.1
7	15573	14.8	6.50	6.50	3.16	462.6	41.33	46.8

$$QL/K(Taw-Tw) = APrRe^{1-N} \quad (7)$$

The result is

$$Q/Q_{ref} = (AK(Taw-Tw)/L Re^{1-N})/Q_{ref} \quad (8)$$

$$RTo = (Taw-Tw) \quad (9)$$

$$\text{so } Q/Q_{ref} = (AKR/LQ_{ref})ToRe^{1-N} \quad (10)$$

With To proportional to M_{∞}^2

$$T^*/To = (1-.5(-1)M_{\infty}^2) = (1+.2M_{\infty}^2) \quad (11)$$

$$To = (1+.2M_{\infty}^2)T \quad (12)$$

with $K=.054$ BTU/HrFt which is changing and is higher with increased Mach number and viscosity. The recovery factor (R) is equal to .9 and $L=107.5$ feet. In general K uses Sutherland's Law of Viscosity which is

$$\mu = 2.27E-8 T_{\infty}^{1.5} / (T^*+198.6) \quad (13)$$

$$K = Cp\mu/Pr \text{ with } Pr=.74 \text{ and } Cp=.6006 \quad (14)$$

$$\text{or } \mu = \rho_{\infty} V_{\infty} L / Re_{\infty} \quad (15)$$

Placing the known constants into the equation the Q/Q_{ref}

$$Q/Q_{ref} = 67.95 \mu A (1+.2M_{\infty}^2) T_{\infty} Re^{1-N} \quad (16)$$

where for laminar flow $A=.332$ and $N=.5$. For turbulent flow $A=.0296$ and $N=.2$. Using the free stream values at the points of interest, the Q/Q_{ref} values for laminar and turbulent flow were calculated. The results are in Table 1.

Table 3. Method 1. Calculations Using Reynold's Analogy and Sutherland's Law

Log Re	Re	μ (slugs/ ft sec)	Ref.Pt	Qref	Q/Qref Laminar	Q/Qref Turbulent
5.75	39811	2.74E-7	1	60.8	.0235	.1197
6.00	63096	2.79E-7	2	67.4	.0270	.1519
6.125	79265	2.95E-7	3	65.0	.0294	.1805
6.2	91397	3.11E-7	4	62.5	.0316	.2040
6.25	100000	3.18E-7	5	57.6	.0333	.2228
6.39	129643	3.32E-7	6	54.1	.0360	.2655
6.50	158489	3.44E-7	7	46.8	.0410	.3260

Method 2 using the normal shock tables required use of the shock tables in Ref. 13. Using the conditions known at each point upstream of the shock, the tables allowed the values M and the ratios T_2/T_1 and P_{∞}/P_0 to be found. Using the formula from Ref. 7 for stagnation pressure

$$P_{ns} = P_{\infty}(1 + V^2/1716T_{\infty}) \quad \text{in atmospheres} \quad (17)$$

we use this value in Ref. 7 to calculate $\log_{10} \mu_0$ and μ . Using (15), Re is found and used with (16) to find Q/Q_{ret} turbulent. The downstream temperature was also calculated using the freestream condition and the shock table ratio. The list of results is on Table 4.

Method 3 considered the downstream flow prior to the boat tail expansion to be approximately Mach 3. By assuming that the body flap is fixed at +7 degrees the tables in Ref. 13 can be used to determine a value θ . Using that θ , the normal Mach number (M_n) can be found using

$$M_n = 3 \sin \theta \quad (18)$$

The weak/strong shock charts in Ref. 13 and the freestream conditions, the ratio T_{∞}/T_0 and thus T_0 can be found. With the assumed Mach 3 condition the ratio T_1/T_0 and T_1 can be determined the same way. The ratio T_2/T_1 and then T_2 can now be determined using the previously determined values and the tables for the Mach number M_n . The value T^* is now found as is

$$T^* = T_2 + .5(T_w - T_2) + .22(TR - T_2), \quad \text{where } TR = .9T_0$$

Table 4. Method 2. Calculations Using Normal Shock Tables
Rockwell Normal Shock Approach

Ref Pt	Mach #	T_2/T_1 Table	P_{n2} (atms)	μ E-6	T_1 deg R	$Re^{.8}$	Q/Q_{ref} Turbulent
1	26.1	133.4	.0164	3.3	47584	87388	.097
2	24.2	114.8	.0279	3.2	41811	144175	.124
3	21.8	93.4	.0367	3.17	36117	190306	.145
4	20.1	87.5	.0434	3.09	36068	233013	.168
5	18.6	68.2	.0469	3.01	29043	266572	.175
6	16.5	53.9	.0631	2.86	24057	377173	.207
7	14.8	43.5	.0743	2.77	20142	479641	.247

using (13) to find the viscosity and (15) for finding Re the Q/Q_{ref} values can now be determined using equation (16). The values of Q/Q_{ref} can be determined the same way for various changes in body flap deflection by fixing all these deflections at one condition (reference point 5 was chosen). This angle is input into the tables and a new value of θ . The exception to this is when the δ_{BF} angle is 0. Then there is no deflection or shock after the Mach 3 flow. Therefore M_n is equal to 3. The results of these calculations are listed in Table 5.

Method 4 used a pressure ratio relationship and the angle the flap makes with the freestream flow to determine the Newtonian flow initial conditions. This pressure ratio is

$$P_2/P_\infty = (\sin^2 \delta \rho_\infty V_\infty^2 / P_\infty) + 1 \quad (20)$$

$$\text{where } \delta = (\alpha + \delta_{BF} - 7) \quad (21)$$

The flap angle was again fixed at +7 degrees which, due to the boattails slope approximately makes the flap deflection equal to the angle of attack. The shock tables give us P_2/P_∞ . The value P_2 can then be determined. Using this value and the T_1 value from the previous method, the equation

$$\rho_1 = P_2 / RT_2 \quad (22)$$

produces the downstream density. The downstream Mach number M_2 can be found from the tables and velocity V_2 can be expressed

$$V_2 = M_2 a = M_2 (\gamma RT) \quad (23)$$

Reynold's number is determined using (15) using the μ from (13)

Table 5. Method 3. Weak Shock Calculations Using $M_\infty=3$

For Body Flap Deflection +7 deg, $\theta=25$, $Mn=1.27$ and $T_2/T_1=1.172$

Ref Pt	T_∞/T_0	T_0	T_1	T_2	T^*	μ E-6	$Re^{\cdot 8}$	Q/Q_{ref}
1	.0079	45152	16124	18897	15290	2.77	6254	.188
2	.0085	43024	15364	18006	14680	2.71	10238	.239
3	.0122	37202	13285	15570	12947	2.54	14165	.278
4	.0165	33787	12065	14140	11968	2.44	17503	.306
5	.0143	29886	10671	12506	10623	2.30	20553	.331
6	.0180	24806	8858	10382	9566	2.17	29256	.392
7	.0223	20721	7400	8672	7868	1.96	39405	.462

For $M_\infty=18.6$, $T_0=29886$, $T_1=10671$, $T_\infty/T_0=.01425$

Ref Pt	δ_{or}	δ	Mn	T_2/T_1	T_2	T^*	μ E-6	$Re^{\cdot 8}$	Q/Q_{ref}
8	0.0	--	----	.357	10670	10109	2.24	21004	.330
9	3.5	22	1.124	1.078	11503	10343	2.27	20806	.331
10	7.0	25	1.270	1.172	12506	10623	2.30	20553	.331
11	10.5	28	1.410	1.261	13456	10890	2.33	20366	.332
12	14.0	32	1.567	1.365	14566	11206	2.36	20130	.333

previous method. $Re^{.6}$ and Q/Q_{ref} using (16) completes the analysis. The changing body flap calculations are done in a similar manner resulting in a changing M_1 and other downstream values. The resulting Q/Q_{ref} showed very little change with the body flap deflections. The results are shown in Table 6.

Method 5 incorporated the Eckert flat plate formula

$$Q/Q_{ref} = (.0296(RT_o - T_w)(Re_x^{-.2})(T^*/T_\infty)^{.4} \quad (24)$$

$$\times (\rho_\infty V_\infty C_p / 778.3 Pr^{.2/3})(P/P_\infty)^{.8}$$

for turbulent flow with deflection where T^* is using (19) and Re from (15). All values used were the original freestream conditions at the reference points, $Pr=.72$, and $C_p=6006$. The q dot value is then divided by the q_{ref} for that point. The results are in Table 7.

Method 6 used the previous Newtonian calculations for H_s and V with the enthalpy equal to

$$H_s = h_{sm} = V_\infty^2 / 2 = C_p T_o \quad (25)$$

Both methods to obtain H_s were used. Then using a $St=.003$ Q was calculated from the equation derived in Ref 13

$$Q = A Re^{.6} (\mu H_s / x) = A Re^{1.0} (\mu H_s / x) / Re^{.2}$$

$$= A (\rho V x / \mu) (H_s \mu / x) / Re^{.2}$$

$$= .003 \rho V_2 H_s / 778.3 \quad (26)$$

This was then divided by the reference Q_{ref} to obtain the Q/Q_{ref} values. These results are displayed in Table 8.

Table 6. Method 4. Newtonian Flow Analysis

For a body flap deflection of +7 deg and $M = 2.6$

Ref Pt	P_2/P_∞	P_∞	P_2	f_2 E-6	a_2	V_2	$Re^{\cdot P}$	Q/Q_{ref}
1	380.51	.0363	13.82	.43	6738.4	17520	23415	.64
2	324.93	.0722	23.45	.76	6578.0	17103	37173	.85
3	252.52	.1158	29.26	1.10	6116.5	15903	49428	.96
4	278.02	.1624	45.15	1.87	5828.9	15155	75068	1.30
5	213.27	.2049	43.70	2.04	5481.8	14253	80505	1.28
6	166.41	.3450	57.41	3.22	4980.0	12948	11278	1.49
7	134.93	.5133	69.26	4.65	4564.8	11868	15435	1.77

For changing body flap, $M_\infty=18.6$ and $P_\infty=.2049$

Ref Pt	θ deg	P_2/P_∞	P_2	f_2 E-6	a_2	V_2	f_2 E-6	$Re^{\cdot P}$	Q/Q_{ref}
8	34.5	156.01	31.98	1.75	5063	15190	2.24	76545	1.20
9	38.0	184.15	37.73	1.91	5257	14983	2.27	82263	1.29
10	41.5	213.27	43.70	2.04	5482	14253	2.30	80505	1.28
11	44.0	242.59	49.71	2.15	5686	14045	2.33	82263	1.34
12	48.5	272.04	55.74	2.23	5916	13607	2.36	81723	1.36

Table 7. Method 5. Eckert Flat Plate Calculations

Ref Pt.	Q	Q/Qref
1	10.41	.1726
2	15.35	.2277
3	15.50	.2384
4	15.39	.2428
5	13.94	.2421
6	14.06	.2598
7	12.41	.2651

Table 8. Method 6. Calculations For Stanton Number-Enthalpy

Ref Pt.	$H_s = \frac{V_\infty^2}{2 E_8}$	Q	Qref	Q/Qref	$H_s = \frac{C_p T_o}{E_8}$	Q	Q/Qref
1	2.923	8.409	60.8	.1383	2.712	7.802	.1283
2	2.555	12.767	67.4	.1894	2.584	12.913	.1916
3	2.202	14.847	65.0	.2280	2.234	15.060	.2310
4	1.995	21.800	63.5	.3430	2.029	22.167	.3490
5	1.768	19.81	57.6	.344	1.795	20.11	.349
6	1.480	23.78	54.1	.440	1.490	23.94	.440
7	1.212	25.79	46.9	.550	1.245	26.47	.566

Method 7 used the Spalding and Chi technique described in Ref 11. This method assumed that the edge conditions next to the wall and temperature at the point of study are known. From Method 3, T_2 and Re_2 are used as the edge conditions. With the wall temperature known the ratio T_w/T_2 is obtained. From the tables in Ref 11 the values F_c and F_{Re} are found. From F_{Re} , the tables are used again to find F_{Ct} . The result produces the value C_f from

$$C_f = F_{Ct} F_c \quad (27)$$

Table 9 shows the calculated C_t values and there input into the Stanton Number-Enthalpy method.

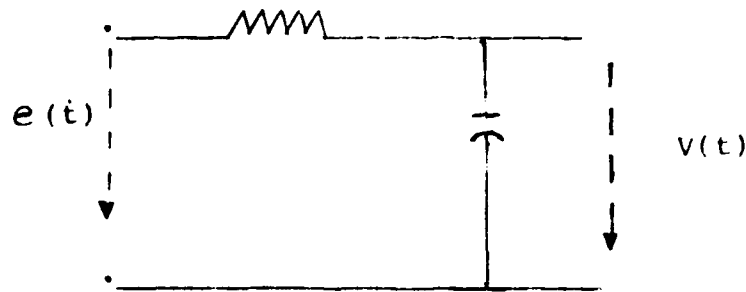
Table 9. Method 7. Calculations of Spalding and Chi Technique
and Its Effect on Stanton Number-Enthalpy Values

Ref Pt.	Tw/Te	Re ₂ E5	Fc	F _{Re}	F _{Re} E6	Re	FcCf	Ct	Q/Qref
1							.0029	.0059	.1380
2							.0029	.0057	.1800
3	.1568	1.55	.52	24	3.71		.0029	.0056	.2120
4							.0029	.0053	.3100
5							.0029	.0050	.3300
6	.26	3.83	.613	10	3.86		.0029	.0047	.3446
7							.0029	.0044	.4200

Appendix 2

RC Circuit Analogy

An RC circuit, excited by a piecewise constant input



If a voltage $e(t)$ is piecewise constant in every interval

$$nT < t < (n+1)T \quad (28)$$

The differential equation is

$$RC \, dV/dt + V = e_n \quad (29)$$

The solution, which equals $V(nT)$ at $t=nT$ is

$$v(t) = e_n + [V(nT) - e_n] e^{-(t-nt)/RC} \quad (30)$$

Evaluating the solution at $t=(n+1)T$, the differential equation becomes

$$V(nT+T) = e_n + [V(nT) - e_n] e^{-(t-nt)/RC} \quad (31)$$

$$V(n+1) = e^{-T/RC} V(n) + (1 - e^{-T/RC}) e_n \quad (32)$$

which is first order linear. Calling $e_n = T_{eq}$, where T_{eq} is the equilibrium temperature related to the heating input

$$T_{eq} = (Q/\epsilon \sigma)^{.25} \quad (33)$$

and $V=T$, the output or thermocouple temperature. The output becomes

$$\text{where } T^n = (1 - e^{-\Delta t/RC}) T_{eq} + e^{-\Delta t/RC} T^{n-1} \quad (34)$$

this is constant at each Δt . This equation could be used to simulate thermocouple temperature for a prescribed heat rate Q corresponding to a given T_{eq} . Solving for T_1

$$(1 - e^{-\Delta t/RC}) T_{eq} = T_1 - [1 - (1 - e^{-\Delta t/RC})^{n-1}] T \quad (35)$$

$$\text{or } T_1 = T_n / [1 - e^{-\Delta t/RC}] - [1 / (1 - e^{-\Delta t/RC}) - 1] T \quad (36)$$

rearranging

$$T_{eq}(tn) = (1 / 1 - e^{-\Delta t/RC}) T_1 - e^{-\Delta t/RC} T_1 (tn-1) \quad (37)$$

$$\text{if } g = 1 / [1 - e^{-\Delta t/RC}] \quad (38)$$

$$\text{then } T_{eq}(tn) = g T_1 - (g-1) T_1 (tn-1) \quad (39)$$

This is the circuit analogy used to calculate an equilibrium temperature. If $g=1$, then you have just the equilibrium assumption. The maximum value of g is assumed to be 3.5 for 1 second of time and the limit of t is $RC \times 1$.

Vita

John Robert Wood was born on 3 May 1952 in Montour Falls, New York. He graduated from Odessa-Montour Central high school in 1970 and attended Corning Community College from which he received an Associate in Science degree in Math-Science in 1972. Later, he received a Bachelor of Science degree in Aerospace Engineering in May 1975. He received a commission in the USAF through the OTS program in July 1976. He served as Chief of Command Engineering and Systems Manager for a low-altitude satellite program under the direction of the Secretary of the Air Force Special Projects at Sunnyvale AFS, California. In 1978 he then served as Sunnyvale AFS Chief, Shuttle Operations Team that supported the first Space Shuttle mission. Capt Wood served at this position until entering the School of Engineering, Air Force Institute of Technology, in June 1981. Upon completion of studies at AFIT, Capt. Wood will be working at Los Angeles AFS, California to the Shuttle Operations office coordinating flight requirements and preparations of Space Division missions flying on the shuttle. Upon completion of work at AFIT, Capt. Wood has been assigned to Los Angeles AFS, California, where he will be working in the Shuttle Operations office (Y00) coordinating flight preparations of Space Division missions flying aboard the shuttle.

Permanent address: 8005 Hill Road
Montour Falls, NY 14865

UNCLASSIFIED

SECURITY CLASSIFICATION OF THIS PAGE (When Data Entered)

REPORT DOCUMENTATION PAGE		READ INSTRUCTIONS BEFORE COMPLETING FORM
1. REPORT NUMBER AFIT/GA/AA/82D-12	2. GOVT ACCESSION NO. AD-A124844	3. RECIPIENT'S CATALOG NUMBER
4. TITLE (and Subtitle) BODY FLAP HEAT TRANSFER DATA FROM SPACE SHUTTLE ORBITER ENTRY FLIGHT TEST MANEUVERS		5. TYPE OF REPORT & PERIOD COVERED MS Thesis
7. AUTHOR(s) John R. Wood Capt. USAF		6. PERFORMING ORG. REPORT NUMBER
9. PERFORMING ORGANIZATION NAME AND ADDRESS Air Force Institute of Technology (AFIT/EN) Wright-Patterson AFB, Ohio 45433		8. CONTRACT OR GRANT NUMBER(s)
11. CONTROLLING OFFICE NAME AND ADDRESS		10. PROGRAM ELEMENT, PROJECT, TASK AREA & WORK UNIT NUMBERS
13. NUMBER OF PAGES 82		12. REPORT DATE December 1982
14. MONITORING AGENCY NAME & ADDRESS (if different from Controlling Office)		15. SECURITY CLASS. (of this report) Unclassified
16. DISTRIBUTION STATEMENT (of this Report) Approved for public release; distribution unlimited		15a. DECLASSIFICATION/DOWNGRADING SCHEDULE
17. DISTRIBUTION STATEMENT (of the abstract entered in Block 20, if different from Report)		
18. SUPPLEMENTARY NOTES Approved for public release; LAW AFR 180-27 LYNN E. WOLAVER Dean for Research and Professional Development Air Force Institute of Technology (AFIT) Wright-Patterson AFB OH 45433 4 JAN 1983		
19. KEY WORDS (Continue on reverse side if necessary and identify by block number) Shuttle Reentry Heating HEATEST Program Orbiter Flight Test Maneuvers		
20. ABSTRACT (Continue on reverse side if necessary and identify by block number) The Space Shuttle Orbiter has conducted various flight maneuvers during the Orbital Flight Test Program in order to establish heating rates at various angles of attack and center of gravity positions. The objective of this project was to investigate the heating effects on the body flap during the entry flight test maneuvers and determine the limits on the flap deflections for an aft center of gravity envelope on the Orbiter.		

DD FORM 1 JAN 73 1473 EDITION OF 1 NOV 65 IS OBSOLETE

SECURITY CLASSIFICATION OF THIS PAGE (When Data Entered)

→ This program available from the Air Force Flight Test Center, AFOTC, uses applicable simulation equations for the simulation performance of the TPS in their flight simulator and simulation program (HEATEST). The approach was to use the HEATEST program to determine the heating on one critical point on the flap during the STS-2 entry flight test inputs (flap temperature #V07T2508). From these results and other results on the outboard elevons, the maximum flap deflection angle and center of gravity could be established.

From the HEATEST program, results were obtained for angle of attack and body flap deflection effects but difficulty was encountered with Reynold's number effect. Several theoretical approaches were investigated resulting in at least one technique that could be applied to HEATEST to linearize or eliminate the Reynold's number effect.

END

FILMED

3-83

DTIC